OPEN ACCESS Freely available online

PLOS ONE

# The Dimethylsulfide Cycle in the Eutrophied Southern North Sea: A Model Study Integrating Phytoplankton and Bacterial Processes

**Nathalie Gypens[1]*, Alberto V. Borges[2], Gaelle Speeckaert[1], Christiane Lancelot[1]**

**1** Ecologie des Systèmes Aquatiques, Université Libre de Bruxelles, Brussels, Belgium, **2** Unité d'Océanographie Chimique, Université de Liège, Liège, Belgium

## Abstract

We developed a module describing the dimethylsulfoniopropionate (DMSP) and dimethylsulfide (DMS) dynamics, including biological transformations by phytoplankton and bacteria, and physico-chemical processes (including DMS air-sea exchange). This module was integrated in the MIRO ecological model and applied in a 0D frame in the Southern North Sea (SNS). The DMS(P) module is built on parameterizations derived from available knowledge on DMS(P) sources, transformations and sinks, and provides an explicit representation of bacterial activity in contrast to most of existing models that only include phytoplankton process (and abiotic transformations). The model is tested in a highly productive coastal ecosystem (the Belgian coastal zone, BCZ) dominated by diatoms and the Haptophyceae *Phaeocystis*, respectively low and high DMSP producers. On an annual basis, the particulate DMSP (DMSPp) production simulated in 1989 is mainly related to *Phaeocystis* colonies (78%) rather than diatoms (13%) and nanoflagellates (9%). Accordingly, sensitivity analysis shows that the model responds more to changes in the sulfur:carbon (S:C) quota and lyase yield of *Phaeocystis*. DMS originates equally from phytoplankton and bacterial DMSP-lyase activity and only 3% of the DMS is emitted to the atmosphere. Model analysis demonstrates the sensitivity of DMS emission towards the atmosphere to the description and parameterization of biological processes emphasizing the need of adequately representing in models both phytoplankton and bacterial processes affecting DMS(P) dynamics. This is particularly important in eutrophied coastal environments such as the SNS dominated by high non-diatom blooms and where empirical models developed from data-sets biased towards open ocean conditions do not satisfactorily predict the timing and amplitude of the DMS seasonal cycle. In order to predict future feedbacks of DMS emissions on climate, it is needed to account for hotspots of DMS emissions from coastal environments that, if eutrophied, are dominated not only by diatoms.

**Citation:** Gypens N, Borges AV, Speeckaert G, Lancelot C (2014) The Dimethylsulfide Cycle in the Eutrophied Southern North Sea: A Model Study Integrating Phytoplankton and Bacterial Processes. PLoS ONE 9(1): e85862. doi:10.1371/journal.pone.0085862

**Editor:** Douglas Andrew Campbell, Mount Allison University, Canada

**Received** September 19, 2013; **Accepted** December 3, 2013; **Published** January 17, 2014



**Funding:** The present work is a contribution to the Fonds de la Recherche Fondamentale Collective DMS-SNS project (1882638) funded by the Fonds de la Recherche Scientifique. The funders had no role in study design, data collection and analysis, decision to publish, or preparation of the manuscript.

**Competing Interests:** The authors have declared that no competing interests exist.

* E-mail: ngypens@ulb.ac.be

## Introduction

Dimethylsulfide (DMS) is a volatile sulfur (S) compound that plays an important role in the global S cycle and may control climate by influencing cloud albedo through the emission of atmospheric aerosols [1]. However, the significance of this feedback remains uncertain [2], as the present knowledge of mechanisms controlling DMS production is insufficient to allow a realistic description of DMS(P) production in Earth System models [3], and predict with confidence the impact of future climate change on surface ocean DMS [4], [5], [6].

In marine ecosystems, phytoplankton are the primary producers of dimethylsulfoniopropionate (DMSP), the precursor of the DMS (e.g. [7]). However, the amount of DMSP synthesized by cells varies among phytoplankton classes and species [8], [9], as well as with the physiological status [10], [11]. Overall, Bacillariophyceae (diatoms) synthesize less DMSP than Dinophyceae and Haptophyceae [8]. The metabolical role of DMSP in marine organisms is still unclear [7]. DMSP has been suggested to play a role as an osmoprotectant [12], [13], as a cryoprotectant [14], [15], [16], and as a nitrogen salvage mechanism during growth limitation [11], [17]. The DMS and/or acrylic acid derived from DMSP cleavage might also act for phytoplankton as an antioxidant [18], [19], [20], as a deterrent for zooplankton [21], [22], [23], or as an anti-viral [24]. The conversion of DMSP to DMS and acrylic acid is catalysed by phytoplankton DMSP-lyases [25]. The intracellular DMSP is also released in the water column as dissolved DMSP (DMSPd) through various phytoplankton mortality processes, including cell lysis [26], [27], grazing pressure [22], [28], and viral infection [29]. Once in the water column, DMSPd is available for assimilation and degradation by bacterioplankton and part of the DMSPd is cleaved into DMS through bacterial metabolism [30], [31], [32]. Although largely variable, phytoplankton and bacterial lyases might contribute almost equally to the DMS production in marine ecosystems [7], [33], [34]. Yet, the main part of DMSPd is degraded by bacteria through the demethylation/demethiolation pathways for fulfilling their S and/or carbon (C) needs [35]. Once produced, DMS can also be consumed by bacteria to satisfy S and mainly C needs [36], photooxided [37], [38], or emitted to the atmosphere across the air-sea interface [39], [40]. The relative importance of these processes is variable and depends on physical forcing factors, but observational evidence suggests that microbial

consumption and photooxidation are the main DMS fates [38], [41], [42]. Because DMS production results from the balance of several complex processes, the link between DMSP production and atmospheric DMS emission is not direct and statistical relationships between DMS concentrations and other environmental variables (such as chlorophyll a (Chl *a*), nutrients, irradiance or mixed layer depth) are uncertain and generally regional in scope [39], [40].

Several mechanistic models of different biological complexity (reviewed by Le Clainche et al. [43]) have been therefore developed to better assess and understand DMS production and controlling factors in marine ecosystem [44], [45], [46], [47], [48], [49], [50], [51], [52], [53], [54], [55], [56], [57], [58]. All these models couple a biogenic S module composed of two or three state variables (DMS, particulate DMSP (DMSPp) and/or DMSPd) to a C- or nitrogen- (N) based ecological model of the plankton community [43], [59]. Most of them subdivide phytoplankton into several functional groups characterized by a specific DMSP cell quota (S:C) in agreement with observations [7]. S:C quota is generally considered as a constant with the exception of models of Le Clainche et al. [52] and Polimene et al. [58] that include variation of S:C with light intensity. The representation of heterotrophic compartments is generally less complex [43] and only some recent modelling studies include an explicit representation of the bacteria (e.g. [50], [56], [57], [58]). To the best of our knowledge the DMSP/DMS model of Archer et al. [50] is the only attempt to link the DMSP/DMS fate to bacterial degradation of organic matter, distinguishing between C and DMS- and DMSP-consuming bacteria types. These authors conclude that a tight coupling between the ecological processes and the DMS cycle is required to properly model DMS emissions to the atmosphere due to both the species dependence of DMSP production and the complexity of microbial metabolic pathways leading to the production of DMS.

Accordingly, we integrated a module describing the DMS(P) cycle into the existing ecological MIRO model [60] that describes C and nutrients cycles in the Southern North Sea (SNS) with an explicit description of the phytoplankton and bacteria dynamics to study the microbial controls of DMS(P) production and fate including DMS emission to the atmosphere. The MIRO model is a conceptual model of the biogeochemical functioning of marine ecosystem that includes an explicit description of growth and fate of *Phaeocystis* (Haptophyceae) that is one of the most intense DMSP producers [8], [61], [62]. The model was applied to the English Channel and the SNS with a focus to the Belgian coastal waters characterized by massive spring blooms of *Phaeocystis globosa* that develops between the spring and summer diatom blooms (e.g. [63], [64], [65]) in response to excess $NO_3^-$ river inputs [66]. This is an adequate case study of *Phaeocystis*-dominated coastal area where the model can be applied to study the link between DMSP production/cleavage by phytoplankton, DMS(P) bacterial transformation, and DMS emissions as field observations also report important DMS concentration [33], [67], [68]. The NE Atlantic Shelves (including the SNS) were indeed pointed as "hot-spot" areas for DMS concentrations (with the Atlantic Subarctic region) in the Atlantic Ocean [40].

In this paper, we first describe the concepts behind the DMS(P) mathematical model and its coupling with the ecological MIRO model (MIRO-DMS). The model is then applied in the SNS to describe the seasonal evolution of DMS(P) and the associated DMS emission to the atmosphere, and provide an annual budget of DMS(P) fluxes. Sensitivity tests on parameters are conducted to identify key microbial controls of DMS(P) production and how these change the emission of DMS to the atmosphere. Finally, we test the applicability of several published empirical relationships that predict DMS from other variables such as Chl *a*.

## Materials and Methods

### Model description

The MIRO-DMS model results from the coupling between a module describing the DMS(P) dynamics and the existing ecological MIRO model developed to represent the dynamics of the ecosystem of the North Sea dominated by *Phaeocystis* colonies [60], [69].

The ecological MIRO model, describing C, N, phosphorus (P) and silica (Si) cycles, assembles four modules describing the dynamics of three phytoplankton Functional Types (FT; diatoms, nanoflagellates and *Phaeocystis* colonies), two zooplankton FT (meso- and microzooplankton) and one bacteria FT involved in the degradation of dissolved and particulate organic matter (each with two classes of biodegradability) and the regeneration of inorganic nutrients ($NO_3^-$, $NH_4^+$, $PO_4^{3-}$ and $Si(OH)_4$) in the water column and the sediment. Equations and parameters were formulated based on current knowledge of the kinetics and the factors controlling the main auto- and heterotrophic processes involved in the functioning of the coastal marine ecosystem (fully documented by Lancelot et al. [60] and in http://www.int-res.com/journals/suppl/appendix_lancelot.pdf).

The description of the DMS cycle requires the addition of three state variables: DMSPp associated to phytoplankton cells, DMSPd and DMS. Processes and parameters describing the DMS(P) cycle (Fig. 1) and its link with carbon rates in MIRO are described below by equations 1 to 12.

**DMSPp synthesis and fate.** The DMSPp is a constitutive compatible solute produced by phytoplankton cell [11]. In the MIRO-DMS model, the DMSPp cellular production and fate are similar to those of other phytoplankton functional molecules, with DMSPp production linked to phytoplankton growth, and DMSPp loss mainly resulting from cell lysis, micro/mesozooplankton grazing and sedimentation (Eq. 1). These processes are described for each phytoplankton FT (diatoms (DA), nanoflagellates (NF) and *Phaeocystis* colonies (OP) expressed in mgC $m^{-3}$) as in the MIRO model and a specific DMSP:C quota (*SC*) is attributed to the three phytoplankton types. The DMSPp (in mmolS $m^{-3}$) state equation is:

$$\frac{dDMSPp}{dt} = [\mu_n - lysis_n - grazing - sed_n] * SC_n \quad \text{for } n = DA,\ NF \text{ and } OP \tag{1}$$

where $\mu_n$ represents the growth of different phytoplankton types (in mgC $m^{-3}$ $h^{-1}$), $lysis_n$ is the phytoplankton lysis (in mgC $m^{-3}$ $h^{-1}$) ($flux_{1+2}$, Fig. 1) and $SC_n$ is the intracellular phytoplankton S:C quotas (molS:mgC) derived from the literature (Table 1; [7]). $sed_n$ correspond to the loss of DMSPp due to diatoms and *Phaeocystis* colonies sedimentation (in mgC $m^{-3}$ $h^{-1}$) ($flux_4$, Fig. 1). In the model, the sedimentation of nanoflagellates is considered as null. *grazing* is the predation pressure of micro and mesozooplankton on respectively on nanoflagellates (NF) and diatoms (DA) (in mgC $m^{-3}$ $h^{-1}$) ($flux_3$, Fig. 1). *Phaeocystis* colonies (OP) are not subject to grazing [70].

**DMSPd release and fate.** The DMSPd simulated in the water column results from the DMSPp released after phytoplankton lysis and zooplankton grazing. When released, DMSPp remains partly as DMSPd in the water column but is also partly

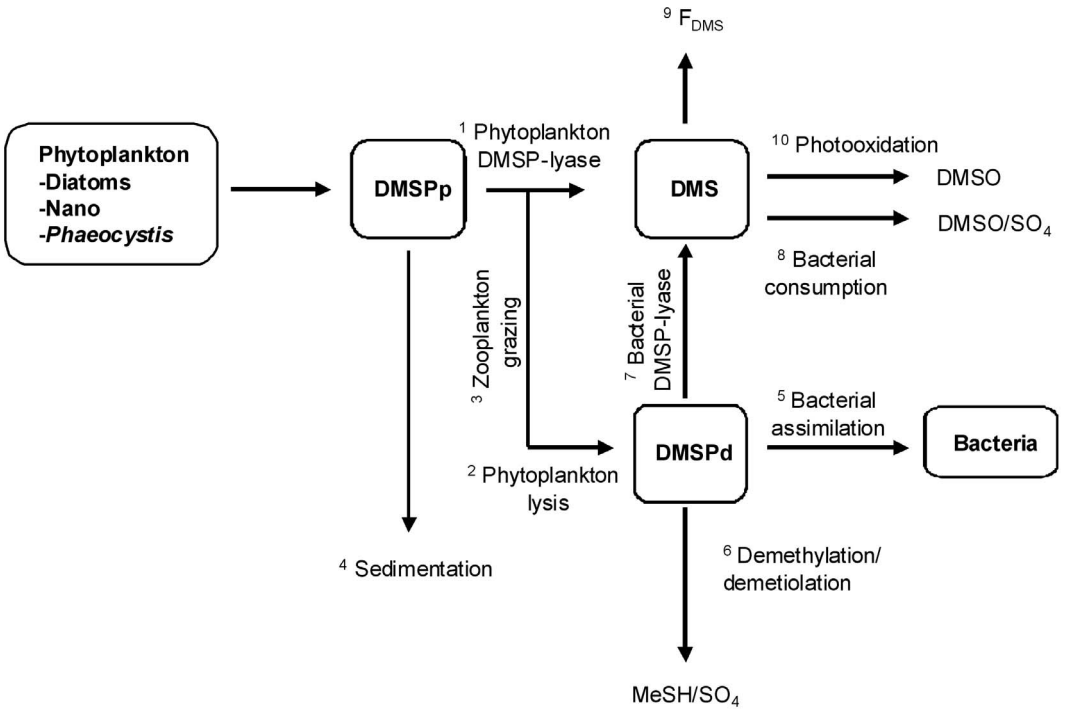


**Figure 1. Diagram representing the state variables and processes of the DMS cycle incorporated into the ecological MIRO model.**
doi:10.1371/journal.pone.0085862.g001

directly cleaved in DMS by phytoplankton DMSP-lyases [22], [25], [61], [71], [72], [73]. The DMSPd originated from micro- and meso-zooplankton grazing is either directly released by "sloppy-feeding", excretion or egestion [21] and can represent up to 70% of the ingested DMSPp [74]. Wolfe and Steinke [22] also suggested that part of the DMSPp is directly converted to DMS. In the model, we assume that all the DMSPp ingested by micro- and meso-zooplankton is transformed into DMSPd (Eq. 1, 2). The fate of DMSPd is controlled by bacteria either through enzymatic cleavage into DMS and/or by demethylation/demethiolation, i.e. the cleavage of DMSPd to methanethiol (MeSH) [75] and acrylate or propionate [76] for fulfilling the C and S needs of bacteria [77], [78]. In the model, the state equation of DMSPd (in mmolS $m^{-3}$) is:

$$\frac{dDMSPd}{dt} = \left(1 - y^{n}_{DMS}\right) * lysis_n * SC_n + grazing * SC_n - DMSPd_{uptake} \qquad for\ n = DA,\ NF\ and\ OP \tag{2}$$

where $y^{n}_{DMS}$ corresponds to the fraction of DMSPp directly cleaved in DMS by phytoplankton DMSP-lyases. In the reference simulation, this fraction was set to 10% of the DMSPp released for each phytoplankton group [34]. $lysis_n$ ($flux_2$, Fig. 1) and *grazing* ($flux_3$, Fig. 1) respectively are the phytoplankton cellular lysis and

**Table 1.** DMS(P) model parameters.

| Parameter | Description | Units | Value | Reference |
|---|---|---|---|---|
| $SC_{DA}$ | Diatoms S:C quota | molS:mgC (molS:molC) | 0.000072 (0.00086) | Stefels et al. [7] |
| $SC_{NF}$ | Nanoflagellates S:C quota | molS:mgC (molS:molC) | 0.00092 (0.011) | Stefels et al. [7] |
| $SC_{OP}$ | *Phaeocystis* colonies S:C quota | molS:mgC (molS:molC) | 0.00092 (0.011) | Stefels et al. [7] |
| $SC_{BC}$ | Bacteria S:C quota | molS:molC | 0.01 | Fagerbakke et al. [103] |
| $y^{DA}{}_{DMS}$ | Part of diatoms DMSPp hydrolysed in DMS by phytoplankton lyase | - | 0.1 | Niki et al. [34] |
| $y^{NF}{}_{DMS}$ | Part of nanoflagellates DMSPp hydrolysed in DMS by phytoplankton lyase | - | 0.1 | Niki et al. [34] |
| $y^{OP}{}_{DMS}$ | Part of *Phaeocystis* colonies DMSPp hydrolysed in DMS by phytoplankton lyase | - | 0.1 | Niki et al. [34] |
| $K0$ | Sea surface photooxydation rate | $h^{-1}$ | 0.09 | Brugger et al. [91] |
| $Ratio^{BC}{}_{S}$ | Bacteria ratio using DMS(P) as substrate for sustain their S need | - | 1 | |

doi:10.1371/journal.pone.0085862.t001

grazing (in mgC $m^{-3}$ $h^{-1}$) and $DMSPd_{uptake}$ is the bacterial uptake of DMSPd (in mmolS $m^{-3}$ $h^{-1}$) ($flux_{5+6+7}$, Fig. 1).

The description of $DMSPd_{uptake}$ is based on the bacterial C uptake described in MIRO, adjusted with the DMSPd stoichiometry of C substrates available to bacteria and taking consideration of the proportion of the bacterial community using the DMSPd (and DMS if necessary) for their C and S needs:

$$DMSPd_{uptake} = Ratio_{BC}^{S} * BC * bmx * \frac{SBC}{SBC + k_{SBC}} * \frac{DMSPd}{SBC} \quad (3)$$

where $Ratio_{BC}^{S}$ is the proportion of the bacterial community using the DMSPd for their S and C need. As a first approximation, we consider in the model that the whole bacterial community is able to degrade DMSP ($Ratio_{BC}^{S} = 1$). *BC* is the bacterial biomass, *bmx* is the bacterial growth, *SBC* are monomeric C substrates available for bacteria and $k_{sbc}$ is the half-saturation constant for the bacterial consumption of *SBC* (in mgC $m^{-3}$).

Bacteria do not assimilate all of the DMSPd they consume, but take only the C and S they need to sustain their growth. It is known that 75 to 90% of DMSPd consumed by bacteria is degraded via demethylation and, although only 5 to 30% of metabolized DMSPd is assimilated into bacterial proteins, and this incorporation could satisfy the total S demands and between 1% and 15% of the C demands of the bacterioplankton [35], [75], [79], [80], [81]. In the model, the bacterial S need (*Sneed*, $flux_5$, Fig. 1) is estimated according to their growth, $Ratio_{BC}^{S}$, and the bacterial S:C ratio, according to:

$$S_{need} = Ratio_{BC}^{S} * BC * y_{BC} * bmx * \frac{SBC}{SBC + k_{SBC}} * SC_{BC} \quad (4)$$

where $y_{BC}$ is the bacterial growth efficiency and $SC_{BC}$ is the bacterial S:C ratio (Table 1).

The DMSPd not assimilated is demethylated (1- $lyase_{Bact}$, $flux_6$, Fig. 1) to produce $SO_4^{2-}$ or MeSH or cleaved by bacterial DMSP-lyase ($lyase_{Bact}$, $flux_7$, Fig. 1) as DMS and acrylate and used for the C requirements of the bacteria [35] according to:

$$bacterial\_lyase = lyase_{Bact} * \left(DMSPd_{uptake} - S_{need}\right) \quad (5)$$

where $lyase_{Bact}$ is the fraction of DMSPd consumed by bacteria which is cleaved in DMS and fixed to 10% for the reference simulation based on Niki et al. [34]. If DMSPd concentration is not sufficient to support bacterial S needs, DMS can be used as S source (Eq. 7) and bacterial DMSP-lyase activity is null.

Beside bacteria, several studies [82], [83], [84] have shown the capacity of some low DMSP-producer phytoplankton taxa to take up DMSPd. Hence, in parallel to their role of DMSP-producer, phytoplankton could also be a sink for DMS(P) cycle and therefore modify atmospheric DMS emission. However, knowledge on the DMSP-uptake phytoplankton taxa, its ecological role and governing factors and the phytoplankton competitive ability for DMSP regarding bacteria uptake is today insufficient for a proper inclusion in the model.

**DMS production and fate.** DMS is produced from enzymatic cleavage of DMSP by phytoplankton [11] and bacteria [85]. The major loss pathways of DMS are the bacterial consumption via the DMS monooxygenase and methyltransferase and oxidation via the DMS dehydrogenase [7], [68], [86], [87], [88]. DMS is also released to the atmosphere [39], [40] or photooxidized into dimethylsulfoxide (DMSO) [37], [38]. The DMS (in mmolS $m^{-3}$) state equation is:

$$\frac{dDMS}{dt} = y_{DMS}^{n} * lysis_n * SC_n + bacterial\_lyase - DMS_{uptake} - photooxydation - F_{DMS} \qquad for\ n = DA,\ NF\ and\ OP \quad (6)$$

where $y_{DMS}^{n}$ corresponds to the fraction of DMSPp directly cleaved in DMS by phytoplankton DMSP-lyases ($flux_1$, Fig. 1), $lysis_n$ is the phytoplankton cellular lysis (in mgC $m^{-3}$ $h^{-1}$), *bacterial_lyase* is the enzymatic cleavage of DMSPd in DMS by bacteria ($flux_7$, Fig. 1), $DMS_{uptake}$ is the bacterial consumption of DMS ($flux_8$, Fig. 1), *photooxidation* term is the photochemical oxidation of DMS into DMSO ($flux_{10}$, Fig. 1) and $F_{DMS}$ is the emission of DMS to the atmosphere through the air-sea water interface (in mmolS $m^{-3}$ $h^{-1}$) ($flux_9$, Fig. 1).

Although bacterial degradation of DMS is important [36], [41], [81], [88] less than 10% of S of DMS consumed is incorporated into bacterial biomass [81], [89] and satisfies 1% to 3% of the bacterial S demand. This suggests that DMS is a minor source of S for bacterioplankton, and is probably taken up by bacteria only as a supplementary substrate [81]. Bacteria predominantly metabolized DMS into non-volatile sulfur products, DMSO and $SO_4^{3-}$ [36], [81], [87], [90].

Based on that, we assume that bacterial uptake of DMS ($DMS_{uptake}$) will cover the bacteria S needs if $DMSPd_{uptake}$ (Eq. 3) is not sufficient. In the model, $DMS_{uptake}$ is described from the consumption of carbon by bacteria and the DMS content of bacterial C substrates, according to:

$$DMS_{uptake} = Ratio_{BC}^{S} * bmx * BC * \frac{SBC}{SBC + k_{SBC}} * \frac{DMS}{SBC} \quad (7)$$

The photooxidation of DMS into DMSO is described considering a photooxidation constant (*K0*, [91]) modulated by the light extinction coefficient in water, according to:

$$photooxidation_z = DMS_z * K0 * \exp^{-kD.z} \quad (8)$$

where *z* is the water depth (m), *K0* is the photooxidation rate in the surface (Table 1; [91]) and *kD* is the light extinction coefficient, and $(DMS)_Z$ is DMS at depth z. As a first approximation, the ultraviolet A (UVA) penetration in the water column is considered equal to that of photosynthetic active radiation (PAR), as PAR attenuation in the studied coastal area is mainly governed by detrital particulate and colored dissolved organic matter. This assumption corresponds to a maximum water penetration of UVA and tends to overestimate the DMS loss by photooxidation.

The DMS air-sea flux ($F_{DMS}$) is determined based on the surface DMS concentration and the gas transfer velocity (*k*) of DMS at in-situ temperature ($k_{DMS}$):

$$F_{DMS} = k_{DMS}[DMS] \quad (9)$$

with

$$k_{DMS} = k_{600}(600/Sc_{DMS})^{0.5} \quad (10)$$

where $k_{600}$ is *k* normalized to a Schmidt number (Sc) of 600 and

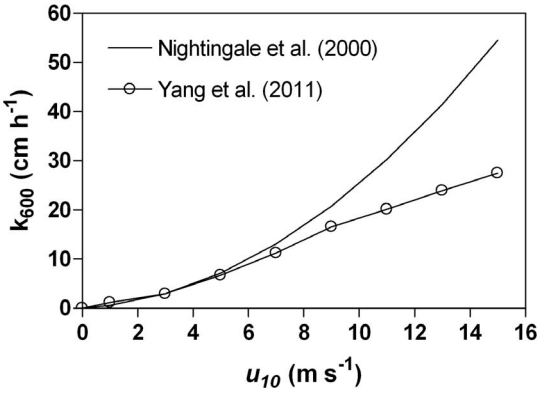


**Figure 2. Gas transfer velocity ($k_{600}$) as a function of wind speed ($u_{10}$) given by the Nightingale et al. [107] parameterization, and the binned measurements of Yang et al. [93] to which was fitted a polynomial relationship (Eq. 13).** The $k$ data of Yang et al. [93] were originally reported normalized to a Schmidt number of 660 ($k_{660}$) and were converted to $k_{600}$.
doi:10.1371/journal.pone.0085862.g002

$Sc_{DMS}$ is the Sc of DMS computed according to Saltzman et al. [92]:

$$Sc_{DMS} = 2674 - 147.12T + 3.726T^2 - 0.038T^3 \qquad (11)$$

where $T$ is sea surface temperature (°C).

$k_{600}$ (cm h$^{-1}$) was computed from a parameterization (Fig. 2) as a function of wind speed referenced at 10 m height ($u_{10}$ in m s$^{-1}$) that we derived from the binned data reported by Yang et al. [93] in their Table 2 (data without bubble normalization):

$$k_{600} = 0.5093u_{10} + 0.2179{u_{10}}^2 - 0.0087{u_{10}}^3 \left(r^2 = 0.999, n = 8\right) \qquad (12)$$

$u_{10}$ data were extracted from the National Centers for Environmental Prediction (NCEP) Reanalysis Daily Averages Surface Flux (http://www.cdc.noaa.gov/) for one station in the North Sea (3.75°E 52.38°N).

## Model implementation

For this application, the MIRO-DMS model was implemented in the SNS using a multi-box 0D frame delineated on the basis of the hydrological regime and river inputs (Fig. 3) [60]. In order to

**Table 2.** $F_{DMS}$ computed for sensitivity tests on DMS(P) model parameters.

| | Parameters | Units | Values | Annual mean [DMS] | $F_{DMS}$ |
|---|---|---|---|---|---|
| | | | | (µmolS m$^{-3}$) | (mmolS m$^{-2}$ y$^{-1}$) |
| **REFERENCE** | | | | **0.9** | **0.19** |
| **Sensitivity to phytoplankton parameters** | | | | | |
| Test 1 | $SC_{NF}$, $SC_{OP}$ | mol S:molC | 0.018 | 1.5 | 0.32 |
| Test 2 | $SC_{NF}$, $SC_{OP}$ | mol S:molC | 0.004 | 0.3 | 0.07 |
| Test 3 | $SC_{DA}$ | mol S:molC | 0.00212 | 0.9 | 0.21 |
| Test 4 | $SC_{DA}$ | mol S:molC | 0 | 0.8 | 0.18 |
| Test 5 | $SC_{DA}$ | mol S:molC | 0.0034 | 1.0 | 0.23 |
| Test 6 | $y^{DA}_{DMS}$, $y^{NF}_{DMS}$, $y^{OP}_{DMS}$ | - | 0 | 0.5 | 0.11 |
| Test 7 | $y^{DA}_{DMS}$, $y^{NF}_{DMS}$, $y^{OP}_{DMS}$ | - | 0.25 | 1.4 | 0.32 |
| Test 8 | $y^{DA}_{DMS}$, $y^{NF}_{DMS}$, $y^{OP}_{DMS}$ | - | 0.5 | 2.4 | 0.53 |
| Test 9 | $y^{NF}_{DMS}$, $y^{OP}_{DMS}$ | - | 0.5 | 2.3 | 0.51 |
| Test 10 | $y^{DA}_{DMS}$ | - | 0.5 | 0.9 | 0.21 |
| **Sensitivity to bacteria parameters** | | | | | |
| Test 11 | $SC_{BC}$ | mol S:molC | 1:37 | 0.8 | 0.17 |
| Test 12 | $SC_{BC}$ | mol S:molC | 1:196 | 0.9 | 0.2 |
| Test 13 | $Ratio_{BC}$ | - | 0.75 | 1.1 | 0.24 |
| Test 14 | $Ratio_{BC}$ | - | 0.5 | 1.4 | 0.32 |
| Test 15 | $Ratio_{BC}$ for DMSPd | - | 0.5 | 0.9 | 0.2 |
| Test 16 | $Ratio_{BC}$ for DMS | - | 0.5 | 1.4 | 0.32 |
| Test 17 | khydrolysis | - | 0.25 | 1.6 | 0.35 |
| **Sensitivity to wind speed and k parameterization** | | | | | |
| Test 18 | wind forcing | m s$^{-1}$ | 3.9 | 0.9 | 0.24 |
| Test 19 | wind forcing | m s$^{-1}$ | −25% | 0.9 | 0.13 |
| Test 20 | wind forcing | m s$^{-1}$ | +25% | 0.9 | 0.26 |
| Test 21 | k parameterization | cm h$^{-1}$ | Nightingale et al., 2002 | 0.9 | 0.19 |

doi:10.1371/journal.pone.0085862.t002

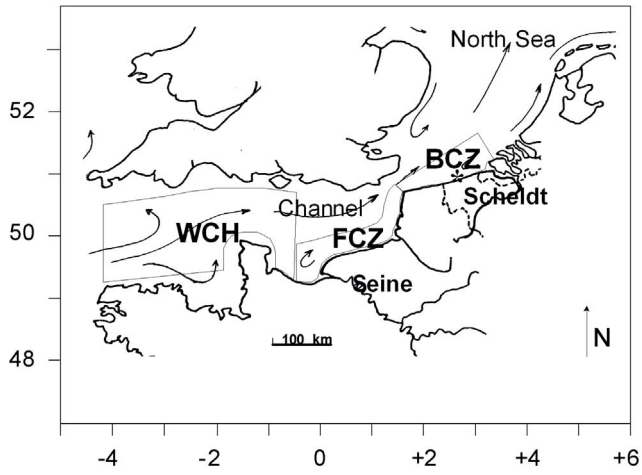


**Figure 3. Map of the study area with the MIRO-DMS multi-box frame delimitation with WCH = Western Channel; FCZ = French Coastal Zone; BCZ = Belgian Coastal Zone (adapted from Gypens et al. [94]).** Model results analysis will focus on the BCZ where simulated results were daily-averaged for year 1989, when DMS(P) field data are available for comparison.
doi:10.1371/journal.pone.0085862.g003

take account for the cumulated nutrient enrichment of Atlantic waters by the Seine and Scheldt rivers, the model was run successively in the Western Channel (WCH) area considered as a quasi-oceanic closed system, the French coastal zone (FCZ) influenced by the Seine and Atlantic waters from the WCH, and, finally, in the Belgian coastal zone (BCZ) influenced by the direct Scheldt loads and the inflowing FCZ waters. Model simulations were performed using meteorological and river forcing for the year 1989 when DMS(P) data are available for comparison [95]. The seasonal variation of the state variables was calculated by solving the different equations expressing mass conservation according to the Euler procedure. A time step of 15 min was adopted for the computation of the numerical integration. The analysis of daily-averaged model results will be performed in the BCZ where field DMS(P) are available [95]. DMS(P) data for the year 1989 were retrieved from the Global Surface Seawater Dimethylsulfide (DMS) Database (available at http://saga.pmel.noaa.gov/dms/) and correspond to data available in the SNS between 51.0°N–52.5°N and 1.5°E–4.5°E [95].

## Results

### DMS(P) seasonal cycle in the Southern North Sea

Validation of the MIRO ecological model is given by Lancelot et al. [60] and Gypens et al. [69], and is not repeated here. The performance of the MIRO-DMS model is evaluated through its ability to reproduce the seasonal variations of available field data of DMSPp, DMSPd and DMS in the BCZ for the year 1989 [95]. However, due to the limited data set, a statistical validation was not attempted and we only compared qualitatively field data and model output. For this comparison, daily simulated results are compared to data of DMS(P) acquired by Turner et al. [67] during short 2–3 day cruises at monthly intervals. Data for each month ranged between 2 and 15 samples, for the purpose of the validation, they were averaged, and standard deviations are given in plots as error bars.

Changes in DMS(P) concentrations are analyzed in parallel to the evolution of the planktonic compartments (phytoplankton and bacteria) (Fig. 4). The phytoplankton evolution simulated in the area is characterized by a succession of spring diatoms, *Phaeocystis* colonies, and summer diatoms (Fig. 4a). Spring diatoms initiate the phytoplankton bloom in early March and are followed by *Phaeocystis* colonies which reach Chl *a* concentration of 25 mgChl*a* $m^{-3}$ (Fig. 4b) in April. Summer diatoms bloom after the *Phaeocystis* decline and remain until fall. On an annual scale, diatom and *Phaeocystis* biomass are similar, the latter being however concentrated during a short period of time, of 1 month (Fig. 4a). In association with the decline of the different phytoplankton blooms, three bacterial maxima are simulated (Fig. 4c).

In agreement with available data, the simulated DMS(P) concentrations show low values except during the spring *Phaeocystis* bloom (Fig. 4d). Simulated DMS(P) values are lower than observed DMS(P) concentrations in early April (the spring diatom bloom). As observed by Turner et al. [67], Kwint and Kramer [68] and van Duyl et al. [96] in North Sea coastal waters, DMSP and DMS concentrations increase in spring and decrease in autumn to low winter values. The maxima in DMS(P) concentrations are limited to a period of about 6 weeks (April, May) and concurred with the *Phaeocystis* bloom as also observed by Stefels et al. [33] in the same area. The model correctly reproduces the observed DMSP seasonal pattern, in particular the timing of the seasonal peak. However, the model fails to reproduce amplitude of the seasonal cycle, with simulated maximal DMSPp concentration (580 μmolS $m^{-3}$; Fig. 4d) three times higher than measured concentration. On the other hand, the modeled DMSPd is much lower than the field observations. This could be due to an experimental bias in older data-sets due to cell breakage leading to an over-estimation of DMSPd and an underestimation of DMSPp [97]. Indeed, the maximum simulated total DMSP (DMSPt = DMSPp + DMSPd) of 670 μmolS $m^{-3}$ is close to the maximum observed DMSPt of 730 μmolS $m^{-3}$. This discrepancy could also be due to the low temporal resolution of observations (1 month, [95]), i.e. insufficient to fully capture the dynamics of the system. Indeed, data obtained with a higher sampling frequency (2 samples per week) in the Wadden Sea (Marsdiep) in 1995, show DMSPp concentrations of about 1700 μmolS $m^{-3}$ during a *Phaeocystis* bloom that reached a maximum of 80 $10^6$ cell $L^{-1}$ [96]. In agreement with these observations, the simulated maximum of DMSPp (Fig. 4d) coincides with the *Phaeocystis* colonies bloom (Fig. 4a) and reach a value of about 580 μmolS $m^{-3}$ for a *Phaeocystis* biomass of 1600 mgC $m^{-3}$ (Fig. 4a) corresponding to 58 $10^6$ cell $L^{-1}$. Hence, the modeled DMSP seasonal peak is bracketed by the lower values of Turner et al. [95] in the more open water of the SNS and the higher values of van Duyl et al. [96] in the near-shore coastal waters of the SNS.

The time lag of about 10 days between the simulated DMSPp and DMSPd (210 μmolS $m^{-3}$; Fig. 4e) peaks is due to the fact that DMSPd results from the phytoplankton lysis and grazing by zooplankton that increase at the end of the bloom. As for DMSPp, simulated DMSPd is also underestimated in comparison with the observed concentration in March during the spring diatom bloom.

The simulated DMS peak reaches a value of 28 μmolS $m^{-3}$ (Fig. 4f) and appears in between DMSPp and DMSPd maxima. The accumulation of DMS simulated during the decay of *Phaeocystis* (Fig. 4a) is consistent with the work of Stefels and van Boekel [61] showing that phytoplankton lyases are active during the stationary phase of the bloom. Simulated and observed DMS show similar seasonal patterns but simulated concentration of DMS is lower than the maxima observed in May (50 μmolS $m^{-3}$, Fig. 4f). However, when spatially averaged over the SNS to take into account for the non-regular distribution of sampling stations, observed DMS concentrations show a maximal value of 25 μmolS $m^{-3}$ (Fig. 5 in Turner et al. [95]).

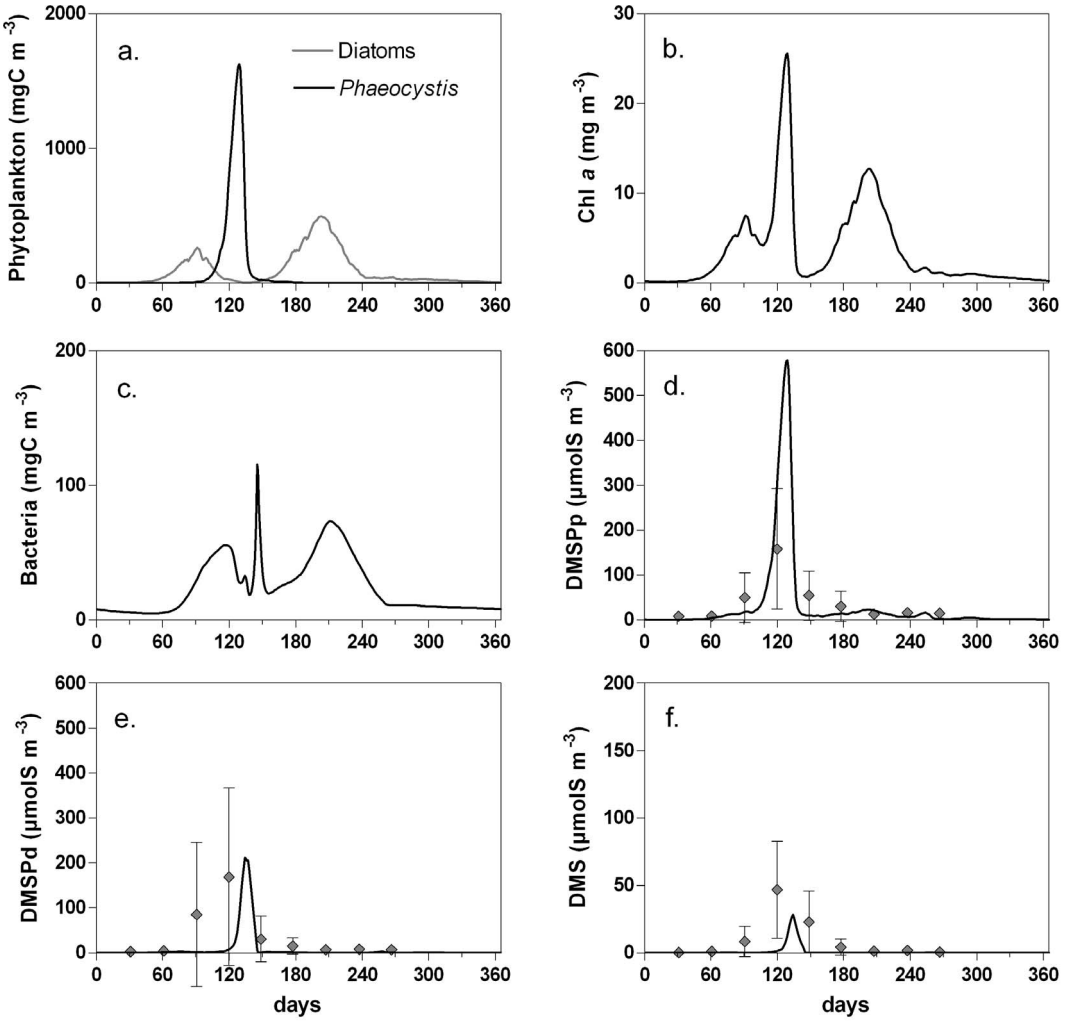


**Figure 4. Seasonal evolution of diatoms and *Phaeocystis* colonies biomass (a), total chl a (b), bacteria biomass (c) and DMSPp (d), DMSPd (e) and DMS (f) concentration simulated for year 1989 in the Belgian Coastal Zone by the MIRO-DMS model and compared to monthly DMS(P) averaged data (◇) from Turner et al. [95].** The error bars represent the standard deviation of the mean.
doi:10.1371/journal.pone.0085862.g004

Figure 5a shows the seasonal evolution of atmospheric DMS emissions simulated by the model in the BCZ. As expected the DMS flux to the atmosphere follows closely the temporal pattern of the simulated DMS concentrations (Fig. 4f), ranging from low values in winter to a maximal value of 37 µmolS $m^{-2}$ $d^{-1}$ in spring. The important daily variability simulated during $F_{DMS}$ peak (Fig. 5a) results from wind speed variability (Fig. 5b).

## Annual DMS budget

The relative importance of each processes involved in the DMS cycle was estimated based on the annual S budget (Fig. 6) obtained by integrating the daily S rates simulated by the model in the BCZ (Fig. 2) and integrated on the average depth of the study area (17 m).

MIRO-DMS estimates the total annual phytoplankton production of DMSPp at 50 mmolS $m^{-2}$ $y^{-1}$, of which 13% are produced by diatoms, 9% by nanoflagellates and 78% by the *Phaeocystis* colonies. From this, 3.2 mmolS $m^{-2}$ $y^{-1}$ of DMSPp are directly converted in DMS by phytoplankton DMSP-lyase (mainly that of *Phaeocystis*) representing a DMS flux similar to bacterial DMSP-lyase activity. The importance of phytoplankton DMSP-lyase was previously reported in the area by Stefels and Dijkhuizen [25] and Wolfe and Steinke [22]. The production of DMS by phytoplankton DMSP-lyase simulated in the model is three times higher than the DMS loss due to flux to the atmosphere and photochemical oxidation, as observed (between 1.5 to 4.5 times) in the Dutch coast during a *Phaeocystis* bloom [33].

DMSPd results from phytoplankton cell lysis (68%) and zooplankton grazing (32%). The dominant process is the cell lysis of *Phaeocystis*, which in itself releases almost 50% of DMSPp throughout the year. The sedimentation of DMSPp amounts to 4.3 mmolS $m^{-2}$ $y^{-1}$. Bacterial uptake accounts for the majority the removal of both DMSPd and DMS inducing a rapid decrease of their concentrations in the water column. The consumption of DMSPd is sufficient to sustain the total bacteria S need (10.8 mmolS $m^{-2}$ $y^{-1}$), and provides up to 16% of bacteria C requirements. In agreement with previous findings [35], [75], [80], [98], the major fate for simulated DMSPd is the demethylation/demethiolation pathways that consumes 28.5 mmolS $m^{-2}$ $y^{-1}$ and results in S products other than DMS (mainly $SO_4^{2-}$ and MeSH). Although only 8% (3.2 mmolS $m^{-2}$ $y^{-1}$) of the DMSPd consumed by bacteria is cleaved to DMS, this flux represents 50% of annual

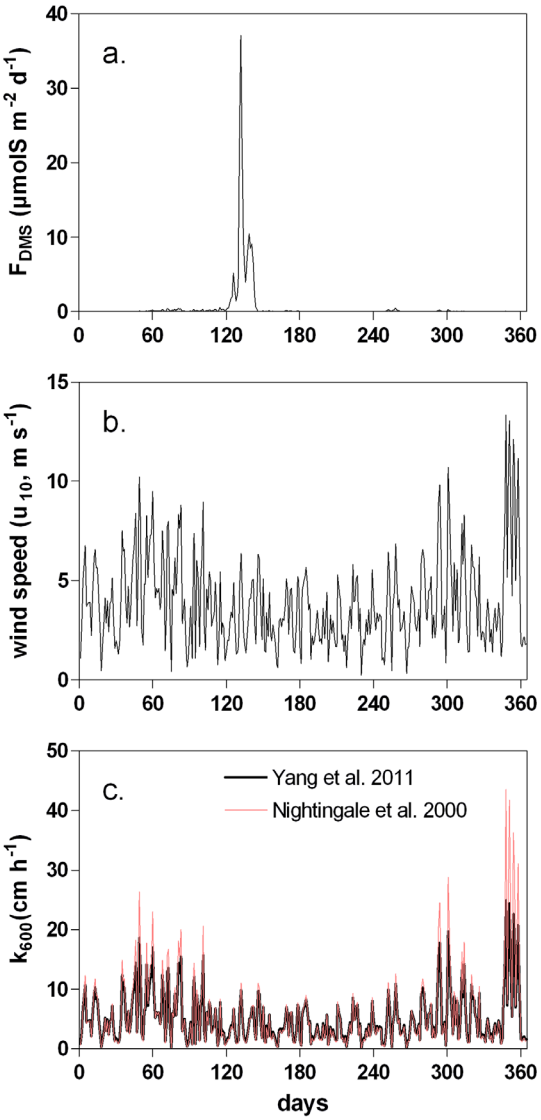


**Figure 5. Daily DMS emission (µmolS m$^{-2}$ d$^{-1}$) computed by the MIRO-DMS model in the Belgian Coastal Zone for year 1989 (a), wind speed ($u_{10}$) (b) and the gas transfer velocity ($k_{600}$) computed using the Yang et al. [93] and the Nightingale et al. [107] relationships (c).**
doi:10.1371/journal.pone.0085862.g005

DMS input and is similar to phytoplankton DMSP-lyase activity (Fig. 6).

Bacteria also consume directly DMS and about 83% (5.3 mmolS m$^{-2}$ y$^{-1}$) of the DMS pool is consumed by bacteria and transformed in $SO_4^{2-}$ or DMSO. Kiene and Bates [41] found that microbial DMS consumption was generally 10 times faster than the flux of DMS to the atmosphere. This ratio is about 17 times in our model results with about 14% of the DMS converted into DMSO by photooxidation and finally only 3% of the DMS emitted to the atmosphere. Annual $F_{DMS}$ represents <1% of the DMSPp production in the water column in agreement with Archer et al. [49].

## Discussion

Annual S budget simulated in the BCZ points both phytoplankton and bacteria as key controlling factors of the DMS production. However the relative importance of these processes will results from their description and parameterization in the model. Sensitivity analyses were then carried out to estimate the impact on the atmospheric emission of DMS of the description of several biological processes compared to physical processes (wind speed and $k_{600}$ parameterization). In particular, the impact of phytoplankton S:C quota determining the maximal DMSP production of the ecosystem, the importance of phytoplankton DMSP-lyase that represents the direct transformation pathway of DMSP into DMS and the DMS(P) bacterial uptake and lyase activity were tested.

### Sensitivity to biological processes

**Sensitivity to phytoplankton parameters.** In our model, phytoplankton S:C quotas were fixed, corresponding to the mean values of measurements for Haptophyceae and diatoms reported by Stefels et al. [7]. Sensitivity tests were performed by varying the S:C quotas within the range of extreme values reported for each phytoplankton type by Stefels et al. [7] (Table 2). Increasing (decreasing) by 70% the *Phaeocystis* S:C value in the model (Test 1 and 2, Table 2) increases (decreases) simulated DMSP and DMS concentrations (Fig. 7; 8a) and annual $F_{DMS}$ by a similar factor (Table 2) without changing the seasonal pattern. Due to the low value of the tested diatom S:C (Tests 3 and 4; Table 2), any modification has little effect on the simulated DMS(P) (Fig. 7; 8a) and $F_{DMS}$ (Table 2). However, some diatom species are characterized by higher S:C quota [8] as *Skeletonema costatum* that is characteristic of the spring diatoms in the SNS [65]. An additional simulation was performed using S:C quota measured for this species (Test 5; Table 2). Increasing the diatom S:C quota increases annual $F_{DMS}$ (Table 2) but also results in an overestimation of simulated DMSPp in summer (Fig. 7). This suggests that in the SNS, dominant diatoms in spring and summer are characterized by different S:C quotas, and that it is essential to take into account for their specific phytoplankton DMSP content to correctly reproduce seasonal evolution of DMS(P) concentration for different FTs (diatoms versus *Phaeocystis*), but also within a FTs (spring versus summer diatoms).

One of the indirect consequences of the choice of the phytoplankton S:C is the possibility for bacteria to fulfil their S need from the consumption of DMS(P). For low phytoplankton S:C ratio (Tests 2 and 4, Table 2) only 60 to 90% of the bacterial S needs in summer and fall can be sustained by DMS(P). As a consequence, the associated bacterial DMSP-lyase activity is decreased.

In the reference simulation, 10% of the DMSP released after phytoplankton lysis is directly cleaved into DMS leading to a DMS flux (3.2 mmolS m$^{-2}$ y$^{-1}$) similar to the DMS flux that comes from bacterial enzymatic cleavage (Fig. 6). However, the relative importance of both processes varies during the seasonal cycle with maximal phytoplankton DMSP-lyase activity simulated at the maximum of the *Phaeocystis* bloom and bacterial DMSP-lyase activity dominating at the decline of the bloom. As deduced by Stefels et al. [7] from the observations of van Duyl et al. [96] in the North Sea, algal DMSP-lyase activity is more important than bacterial enzymatic cleavage at high concentration of DMSPd and explains the occurrence of maximum DMS concentration before the DMSPd peak in our results (Fig. 4e,f). After the decay of the *Phaeocystis* bloom, bacteria and associated DMSP cleavage largely increase.

Most, but not all [34], DMSP-producing species of phytoplankton have DMSP-lyase activity. However, the importance of this activity is not especially correlated with intracellular DMSP concentration [72], [99]. The importance of the direct

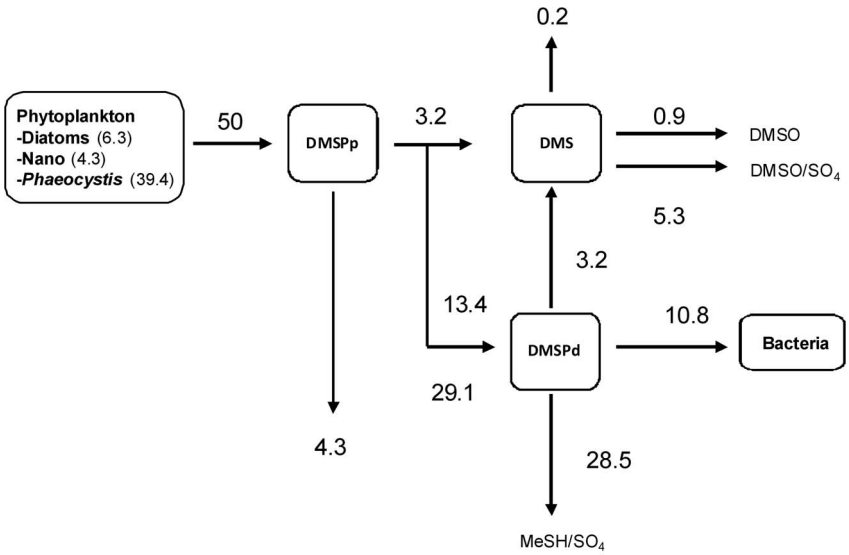


**Figure 6. Annual sulfur budget in the Belgian Coastal Zone computed by the MIRO-DMS model for the year 1989 (mmolS $m^{-2}$ $y^{-1}$).**
doi:10.1371/journal.pone.0085862.g006

transformation of DMSP into DMS, on the DMS emission was tested by varying the cleavage yield ($y^n_{DMS}$, Eq. 3) between 0% and 50% (Table 2). The absence of phytoplankton DMSP-lyase activity (Test 6, Table 2), delays the DMS peak by a few days, and decreases both the simulated DMS (Fig. 8b) and $F_{DMS}$ by about 40% (Table 2). This is higher than the 25% computed by van den Berg et al. [46] based on a modeling study in the SNS. When 25% or 50% of DMSPd released from phytoplankton lysis is converted into DMS (Tests 7 to 9; Table 2), the DMS concentration and $F_{DMS}$ largely increase compared to the reference simulation (from 1.5 to 2.5 times, Table 2). Although simulated DMSPd decreases, this effect is limited as the DMSPd pool is also provided by zooplankton grazing, and its fate controlled by bacterial activity. Increasing only diatom DMSP-lyase yield has little effect on $F_{DMS}$ (Test 10; Table 2), indicating the dominance of *Phaeocystis* in phytoplankton DMSP-lyase activity.

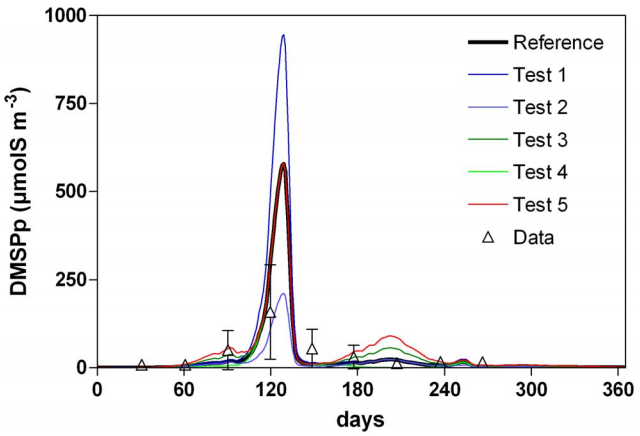


**Figure 7. Seasonal evolution of DMSPp concentration simulated by the MIRO-DMS model for year 1989 for different phytoplankton *S:C* ratio (see Table 2 for the description of the sensitivity tests).**
doi:10.1371/journal.pone.0085862.g007

Altogether these sensitivity tests show that phytoplankton DMSP-lyase is a key process controlling both DMS concentration and $F_{DMS}$ and even more important when associated to a high DMSP-producer such as *Phaeocystis*. It is therefore important to determine this enzymatic activity in high DMSP-producing species or among species that co-occur with high DMSP-producing species. An explicit description of DMSP-lyase activity in models could also be important if this activity varies as a function of environmental conditions.

**Sensitivity to bacteria parameters.** As observed by several authors (e.g. [75]), bacterial uptake is the major fate of DMSPd in the model, but only 8% of this DMSPd is cleaved into DMS by bacteria. This agrees with recent observations concluding that bacteria are not key players in DMSPd cleavage into DMS [100], [101] but play a major role in regulating the flux of DMS indirectly by the consumption and demethylation of DMSPd with production of S product other than DMS.

However, the proportion of DMSPd consumed by bacteria and transformed into DMS is function of the DMSPd concentration [96] and the bacterial S demand [35]. Indeed, previous studies suggested that the fraction of DMSPd converted into DMS increases with DMSPd concentration [75]. Lower DMSPd concentrations are completely assimilated, whereas higher concentrations result in increasing amounts of DMS produced [102]. Moreover, a strong demand for S decreases bacterial cleavage of DMSPd [35]. The sensitivity of model results to DMSPd concentration and/or bacterial S needs was estimated either by modifying the release of DMSPd by phytoplankton, the bacterial S:C quota or the proportion of the bacterial community that use DMSP as S source.

In the model, DMSPd is released in the water column by phytoplankton lysis and grazing processes (Eq. 2). The modification of the phytoplankton DMSP-lyase activity affects the $F_{DMS}$ but also the relative contribution of phytoplankton and bacterial processes to DMS production. Increasing the direct transformation of DMSPp in DMS by phytoplankton DMSP-lyase will decrease the DMSPd bacterial uptake and the bacterial production of DMS. Increasing the cleavage yield ($y^n_{DMS}$, Eq. 3) up to 50% (Test 8, Table 2) will decrease bacterial DMS production by 40% but increases both DMS production by phytoplankton and

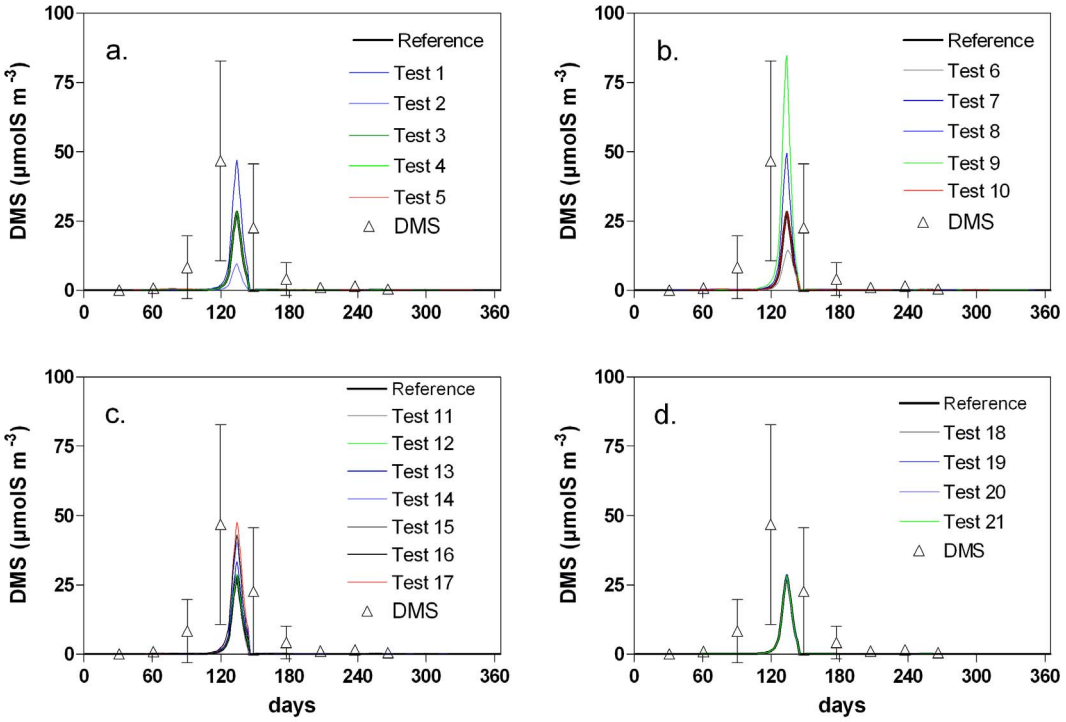


**Figure 8. Seasonal evolution of DMS concentration simulated by the MIRO-DMS model for year 1989 by modifying phytoplankton S:C ratio (a), phytoplankton lyase (b), bacteria S:C content and bacterial processes (c) and wind speed (d).** See Table 2 for the description of the sensitivity tests.
doi:10.1371/journal.pone.0085862.g008

$F_{DMS}$. However, when compared to the data available in the literature [7], [34], these results overestimate the contribution of phytoplankton compared to bacteria to the DMS production (with phytoplankton contribution up to 90% of the DMS production). One possible source of overestimation of DMSPd concentrations in the model can however result from the assumption that all the DMSPp ingested by micro- and meso-zooplankton is transformed into DMSPd (Eq. 1, 2). Indeed, Wolfe and Steinke [22] also suggested that part of the DMSPp can be directly converted to DMS since digestion promotes the activity of DMSP-lyase present in the membrane of the prey. To test the impact of the direct conversion of DMS by zooplankton, 30% of DMSPp (based on Archer et al. [74]) ingested by grazing was directly transformed in DMS and added in Eq. 6. This results in an increase of DMS concentration in the water column and of $F_{DMS}$ (0.29 mmolS $m^{-2}y^{-1}$) with little impact on DMSPd concentration.

Sensitivity tests were then conducted by varying the bacterial S:C quota between extreme values reported in the literature i.e. 1:37 and 1:196 molS:molC ([103]; Tests 11 and 12; Table 2). In our model, decreasing the bacterial S:C ratio will decrease the proportion of consumed DMSPd that will be assimilated by bacteria and increase the cleavage of DMSPd into DMS. This can enhance the $F_{DMS}$. However, as shown in Table 2, this parameter is not very sensitive in our application as the DMSPd produced is largely enough to fulfil the S needs of the whole bacterial community.

In a third series of tests, we modified the percentage of bacteria able to use DMSPd and/or DMS as S source. The hypothesis of 100% used in the reference simulation was based on the observation that most marine bacteria have the genetic capability to demethylate DMSP [36], [104], [105] and that DMSPd/DMS concentrations can support almost all bacteria S needs [79], [80], [87]. However, all bacteria are not able to metabolize DMSP and/or DMS. We therefore explore the sensitivity of the model to the bacteria diversity by decreasing this proportion to 75% or 50% (Tests 13 and 14; Table 2). As expected, the turnover rate of DMSPd and DMS decreases and the $F_{DMS}$ increases (Table 2). The maximum concentrations of DMSPd and DMS (Fig. 7c) simulated are 270 µmolS $m^{-3}$ and 33 µmolS $m^{-3}$ when considering that 75% of the bacterial community is able to degrade DMS(P) and 375 µmolS $m^{-3}$ and 40 µmolS $m^{-3}$ for a fraction of 50%. The simulated DMS emissions to the atmosphere also increase with an annual $F_{DMS}$ of about 0.24 and 0.32 mmolS $m^{-2}$ $y^{-1}$, respectively, compared to 0.19 mmolS $m^{-2}$ $y^{-1}$ in the reference simulation (Table 2). This increase of DMS emission results from the combination of bacterial DMSP cleavage and the decrease of bacterial DMS uptake. In these simulations, bacterial DMSP-lyase activity shows a small increase (up to 3.4 and 3.6 mmolS $m^{-2}$ $y^{-1}$ compared to 3.2 mmolS $m^{-2}$ $y^{-1}$ in the reference simulation), and the increase of $F_{DMS}$ mainly results from the decrease of bacterial DMS uptake and the accumulation of DMS in the water column. This is confirmed by results obtained by modifying only DMSPd (Test 15) or DMS bacterial uptake (Test 16). These results are consistent with the observations that suggest that bacterial DMS uptake may be a quantitatively important sink for DMS from the surface ocean [36], [81], [87], [90].

In the model, bacterial cleavage of DMSP in DMS represents 10% of the uptake of DMSPd not assimilated by bacteria. To test the importance of bacterial DMSP-lyase activity, this fraction was set to 25% inducing an increase of almost two fold of both the concentration of DMS and $F_{DMS}$.

Due to their importance on both DMSPd and DMS transformation, bacterial processes need to be accurately described and/or

parameterized in ecosystem models. Note that in the present version of the model we only considered one bacterial community, and we did not individually represent the DMS- or DMSP-consumers although this simplification also induces possible uncertainties and underestimation of $F_{DMS}$ resulting from the maximal hypothesis of bacterial uptake ($Ratio^{BC}{}_S = 1$). This is particularly important for the direct bacterial uptake of DMS. Similarly, the bacteria state variable lumps both bacteria and Achaea that might also be important for the demethylation/demethiolation processes [106].

## Sensitivity to physical processes: Wind speed and $k_{600}$ parameterization

Besides biological processes, $F_{DMS}$ is also function of the $k_{600}$ that depends on the intensity of wind speed and how it is translated into turbulence (depending on the parameterization). Additional tests were performed to estimate the sensitivity of the simulated atmospheric emission of DMS to wind speed and $k_{600}$ parameterization (Table 2). Changing wind speed will mainly affect the $F_{DMS}$ that change up to 37% (Test 20, Table 2) with little change for DMS concentrations (Fig. 8d). Due to very low values of wind speed (Fig. 5b) during the *Phaeocystis* bloom and the peak production of DMS (Fig. 4a,d), the use of a constant annual mean wind speed will increase annual $F_{DMS}$ (Test 18; Table 2). Indeed, to accurately compute $F_{DMS}$ it is required to use high temporal resolution $u_{10}$ data [49]. However, considering the low effect of $F_{DMS}$ compared to bacterial DMS consumption, this has little impact on the dissolved DMS concentration (Fig. 8d).

In the reference simulation we used a parameterization of $k_{600}$ based on the data reported by Yang et al. [93]. Several other parameterizations of $k_{600}$ exist and for the purpose of a sensitivity analysis, we chose the one of Nightingale et al. [107] that has been used in the recent $F_{DMS}$ climatology of Lana et al. [40]. Nightingale et al. [107] parameterize $k_{600}$ as a function of $u_{10}$, according to:

$$k_{600} = 0.33u_{10} + 0.22u_{10}^2 \quad (13)$$

The $k$ values used in the Nightingale et al. [107] parameterization were determined from two dual tracer ($^3$He and $SF_6$) release experiments in the SNS, and this parameterization has been shown to be also applicable in open ocean conditions [108]. The $k$ values of Yang et al. [93] were obtained from measurements of [DMS] and direct measurements of $F_{DMS}$ by eddy-covariance during 2 experiments in the Pacific Ocean and 3 experiments in the Atlantic Ocean. The $k_{600}$ values of Nightingale et al. [107] and Yang et al. [93] strongly diverge at $u_{10} > 8$ m s$^{-1}$ (Fig. 2). This has been attributed to reduced bubble-mediated transfer at high wind speeds of highly soluble DMS compared to enhanced bubble-mediated transfer of sparingly soluble gases such as $^3$He and $SF_6$.

The net annual $F_{DMS}$ computed with the Yang et al. [93] derived parameterization (Eq. 12) and the Nightingale et al. [107] parameterization (Eq. 13) are not different in the area during the simulation period. This is due to the fact that during the period of high DMS concentrations (during the *Phaeocystis* bloom) wind speed is low (average $3.3 \pm 1.7$ m s$^{-1}$, Fig. 5b), and the $k_{600}$ values computed from the two relationships are very close (Fig. 5c). The two $k_{600}$ relationships only significantly diverge for $u_{10} > 8$ m s$^{-1}$ (Fig. 2), and such $u_{10}$ values only occur during winter and fall in the SNS (Fig. 5b) when [DMS] is very low or zero (Fig. 4f). Since wind speeds $>8$ m s$^{-1}$ are rare events in the area ($<6\%$ of observations), the annual average of $k_{600}$ computed from the Yang et al. [93] relationship (5.20 cm h$^{-1}$) is only $\sim$9% lower than the one computed using the Nightingale et al. [107] relationship (5.67 cm h$^{-1}$).

## Comparison of DMS and $F_{DMS}$ modelled by the mechanistic MIRO-DMS model and derived from empirical relationships (statistical models)

In order to achieve global [109], [110], [111], [112], [113], [114], [115] or regional [116] estimates of $F_{DMS}$, several empirical relationships have been derived from DMS field data and variables such Chl *a*, $NO_3^-$, T, primary production, solar radiation, or mixed layer depth that can be derived at higher spatial and temporal resolution from climatologies, remote sensing or models. We tested if some of these empirical relationships that are assumed universal and generic were applicable to the SNS that is representative of a temperate eutrophied coastal system. Several empirical parameterizations that allow to compute DMS concentration in marine waters (Table 3) were applied in the area using MIRO-DMS outputs (Chl *a*, $NO_3^-$) and compared to DMS concentration obtained with the MIRO-DMS, and with the available DMS observations in area (Fig. 9a).

DMS concentrations simulated with the algorithm of Simó and Dachs [111] show maximal DMS concentrations similar to those simulated by the model during the *Phaeocystis* bloom (Fig. 9a). However, they overestimate $F_{DMS}$ along the seasonal cycle (Fig. 9b), in particular due to an overestimation of the DMS concentrations related to spring and summer diatom blooms (Fig. 9a). Neither Anderson et al. [109] nor Lana et al. [114] relationships can reproduce the amplitude of DMS seasonal cycle and DMS peak associated to *Phaeocystis* bloom (Fig. 9a). As for the Simó and Dachs [111] relationship, the Anderson et al. [109] and Lana et al. [114] relationships over-estimate the DMS concentration associated with the diatom spring and summer blooms. In the area, the mixed layer depth is constant (= total depth, since it is a permanently well-mixed shallow system) and the seasonal evolution of DMS concentrations (Fig. 9a) simulated by all these relationships is controlled by the evolution of Chl *a* (Fig. 9c), without any distinction in DMSP cellular content among phytoplankton groups. To take into account of this variability we also tested two additional relationships respectively developed by Aumont et al. [110] and revised by Belviso et al. [112] based on a similar data-set. The Fp ratio representing the community structure index (and corresponding to the ratio of the diatoms and dinoflagellates to the total Chl *a*) used in these relationship was computed based diatoms and non-diatoms (nanoflagellates and *Phaeocystis* colonies) Chl *a* simulated by the MIRO-DMS model. Results obtained with both relationships largely overestimated DMS concentrations in the area during *Phaeocystis* bloom (with DMS values up to 400 nM with the Belviso et al. [112] equation and unrealistic values up to 5000 nM with the Aumont et al. [110] equation). Both relationships were established from data-sets with total Chl *a* values $<4$ µg L$^{-1}$ (and non-diatom Chl *a* values lower than 1 µg L$^{-1}$), well below the maximum values in the SNS, up to 25 µg L$^{-1}$ (Fig. 4b). Based on these results, we conclude that these relationships are not adapted to ecosystems dominated by high biomass of non-siliceous species, typically in eutrophied coastal environments.

The $F_{DMS}$ computed from DMS derived the various empirical parameterizations are higher than $F_{DMS}$ computed with MIRO-DMS, about 6 times higher for Lana et al. [114] and about 10 to 15 times higher for Anderson et al. [109] and Simó and Dachs [111] relationships. These $F_{DMS}$ values are also largely higher than the maximal $F_{DMS}$ previously estimated in the area [33], [46], [67], [117]. Despite the fact that these relationships give lower

**Table 3.** Empirical relationships tested in the MIRO-DMS, and the corresponding annual mean of [DMS] and $F_{DMS}$. *Fp* is the community structure index computed as the ratio between the diatoms and non-diatoms (nanoflagellates and *Phaeocystis* colonies) Chl *a* simulated by the MIRO-DMS and *z* in the depth of the mixed layer (m) that is constant in the MIRO-DMS application (17m).

| Equations | Reference | [DMS] | $F_{DMS}$ |
|---|---|---|---|
| | | (µmolS $m^{-3}$) | (mmol S $m^{-2}$ $y^{-1}$) |
| [DMS] = 2.29 for log10(CJQ)<1.72 | Anderson et al. [109] | 2.2 | 2.23 for $k_{NO3}$ = 0.8 |
| [DMS] = 8.24 [log10(CJQ)−1.72]+2.29 for log10(CJQ)>1.72 | | 2.5 | 2.63 for $k_{NO3}$ = 2 |
| where C = Chl a ($mgm^{-3}$), J = mean daily irradiance ($Wm^{-2}$) | | | |
| and Q = $NO_3/(NO_3+k_{NO3})$ ($mmolm^{-3}$) | | | |
| [DMS] = −ln (z)+5.7 for Chl a/z<0.02 | Simó and Dachs [111] | 3.1 | 3.03 |
| [DMS] = 55.8 (Chl a/z)+0. for Chl a/z>0.02 | | | |
| [DMS] = 2.356+0.614 * Chla | Lana et al. [114] | 1.1 | 1.21 |
| DMSPp = (20*Chla*Fp)+21 for Chla'<0.3 mg $m^{-3}$ | Belviso et al. [112] | - | - |
| DMSPp = (20*Chla*Fp)+(356.4 * Chla −85.5) | | | |
| for Chla'>0.3 mg $m^{-3}$ | | | |
| DMS:DMSP = 0.231−3.038Fp−16 $Fp^2$ | | | |
| −38.05$Fp^3$+41.12$Fp^4$−16.32$Fp^5$ | | | |
| DMSPp = (20*Chla*Fp)+ | Aumont et al. [110] | - | - |
| (13.64+0.10769* (1+24.97*(1-Fp)*Chla)$^{2.5}$) | | | |
| DMS:DMSP = 0.015316+0.005294/(0.0205+Fp) for Fp<0.6 | | | |
| DMS:DMSP = 0.674*Fp−0.371 for Fp>0.6 | | | |

doi:10.1371/journal.pone.0085862.t003

seasonal maxima DMS concentrations (with the exception of the Simo and Dachs [111] relationship), they compute DMS concentrations through the year during both diatom and *Phaeocystis* blooms. MIRO-DMS only simulates DMS during the *Phaeocystis* bloom, when wind speed and $k_{600}$ are low (Fig. 5b,c), while DMS is very low during the rest of the year.

## Conclusions

The application in the BCZ of the newly developed biogeochemical model MIRO-DMS shows that modelled $F_{DMS}$ is more sensitive to the description and parameterization of biological than abiotic processes. The results confirm the importance of accounting for specific phytoplankton cellular DMSP between different FTs (*Phaeocystis versus* diatoms) but also within a FT (spring *versus* summer diatoms) to describe DMSP and DMS concentrations in marine ecosystems. Due to their elevated S:C quota and their

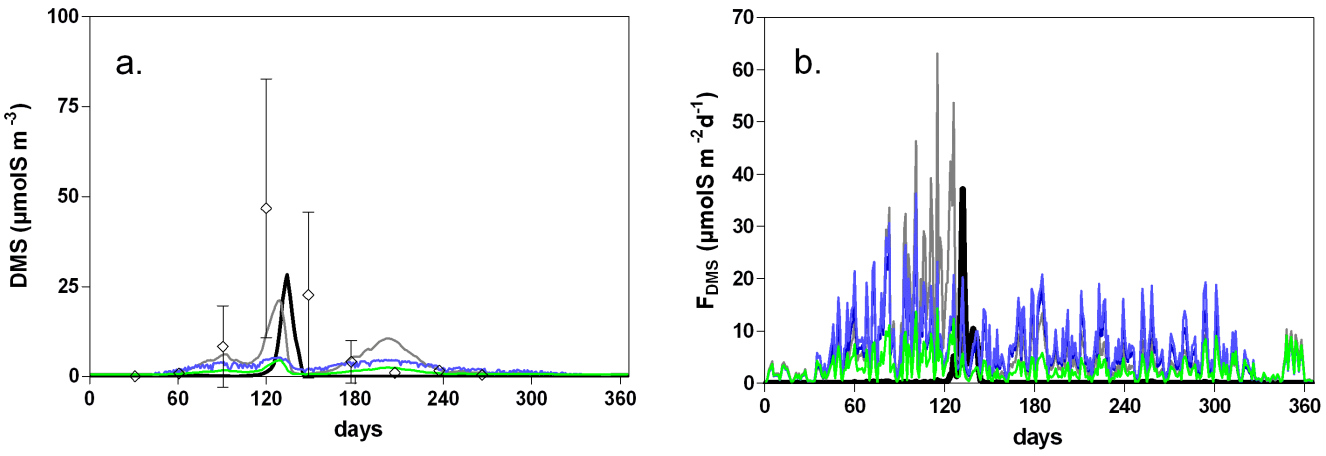


**Figure 9. Seasonal evolution of DMS concentration (a) and flux (b) computed in the BCZ for year 1989 using the MIRO-DMS model (black) and the empiric relationship of Simó and Dachs [111] (grey), Anderson et al. [109] with a $k_{NO3}$ of 0.8 and 2 mmolN $m^{-3}$ (blue) and Lana et al. [114] (green) and compared to available data (◇) from Turner et al. [95].** The error bars represent the standard deviation on the mean.
doi:10.1371/journal.pone.0085862.g009

major contribution (50%) to the annual primary production, *Phaeocystis* colonies are responsible of 78% of the annual production of DMSP in the BCZ. This work is an additional modelling effort to explicitly include bacterial processes in transforming DMS(P), and shows their contribution in processing DMSP and as a sink of DMS that is much higher than DMS removal by photooxidation and $F_{DMS}$.

Current empirical relationships to predict DMS from Chl *a* [109], [110], [111], [112], [114] were unable to satisfactorily reproduce the seasonal cycle of DMS in timing and amplitude in the SNS in comparison with field data and MIRO-DMS simulations. In the data-sets from which these empirical relationships were established, the high Chl *a* values were related to diatoms unlike eutrophied coastal environments such as the SNS where high biomass is not associated to diatoms. Therefore, future projections of $F_{DMS}$ and the investigation of the potential feedback on climate require to use modeling tools that accurately represent DMS(P) dynamics in coastal environments that are hotspots of DMS emissions, in particular, in eutrophied coastal environments dominated by high biomass non-diatom blooms. Further, bacterial processing of DMS(P) needs to be correctly represented in models. The potential feedbacks of DMS emissions on climate will depend on the impact of climate change on the phytoplankton composition and biomass, as postulated by the CLAW hypothesis [1], but also of the response of the bacterial communities to global changes, and how they will modulate the sinks of DMS in seawater (emission to the atmosphere *versus* bacterial consumption/transformation).

## Acknowledgments

We are grateful to Sébastien Milleville for his work during his master thesis. AVB is a senior research associate at the FNRS. We acknowledge two anonymous reviewers and the editor for constructive comments on the manuscript.

## Author Contributions

Conceived and designed the experiments: NG CL AVB. Performed the experiments: NG. Analyzed the data: NG GS AVB CL. Contributed reagents/materials/analysis tools: NG GS AVB CL. Wrote the paper: NG GS AVB CL.

## References

1. Charlson RJ, Lovelock JE, Andreae MO, Warren SG (1987) Oceanic phytoplankton, atmospheric sulphur, cloud albedo and climate. Nature 326:655–661.
2. Quinn PK, Bates TS (2011) The case against climate regulation via oceanic phytoplankton sulphur emissions. Nature, 480, 51–56.
3. Halloran PR, Bell TG, Totterdell IJ (2010) Can we trust empirical marine DMS parameterisations within projections of future climate? Biogeosciences 7:1645–1656. doi:10.5194/bg-7-1645-2010.
4. Cameron P, Elliott S, Malrud M, Erickson D, Wingenter O (2011) Changes in dimethyl sulfide oceanic distribution due to climate change. Geophys Res Lett 38(7), doi: 10.1029/2011GL047069.
5. Levasseur M. (2011) If Gaia could talk. Nature Geosci. 4: 351–352.
6. Six KD, Kloster S, Ilyina T, Archer SD, Zhang K, et al. (2013) Global warming amplified by reduced sulphur fluxes as a result of ocean acidification. Nature Climate Change doi:10.1038/nclimate1981.
7. Stefels J, Steinke M, Turner SM, Malin G, Belviso S (2007) Environmental constraints on the production and removal of the climatically active gas dimethylsulphide (DMS) and implications for ecosystem modelling. Biogeochemistry 83(1-3): 245–275.
8. Keller MD, Bellows WK, Guillard RRL (1989) Dimethyl sulfide production in marine phytoplankton. In: Saltzman ES, Cooper WJ (eds) Biogenic sulfur in the environment. American Chemical Society, Washington DC, pp 167–182.
9. Matrai PA, Keller MD (1994) Total organic sulfur and dimethylsulfoniopropionate in marine phytoplankton: intracellular variations. Mar Biol 119:61–68.
10. Keller MD, Korjeff-Bellows W (1996) Physiological aspects of the production of dimethylsulfoniopropionate (DMSP) by marine phytoplankton. In: Kiene RP, Visscher P, Keller M, Kirst G (eds) Biological and environmental chemistry of DMSP and related sulfonium compounds. Plenum Press, New York, p 131—142.
11. Stefels J (2000) Physiological aspects of the production and conversion of DMSP in marine algae and higher plants. J Sea Res 43:183–197.
12. Vairavamurthy A, Andreae MO, Iverson RL (1985) Biosynthesis of dimethylsulfide and dimethylpropiothetin by Hymenomonas carterae in relation to sulfur source and salinity variations. Limnol Oceanogr 30: 59–70.
13. Dickson DMJ, Kirst GO (1987) Osmotic adjustment in marine eukaryotic algae: The role of inorganic ions, quaternary ammonium, tertiary sulphonium and carbohydrate solutes. I. Diatoms and a Rhodophyte. New Phytologist 106: 645–655.
14. Karsten U, Wiencke C, Kirst GO (1992) Dimethylsulphonio-propionate (DMSP) accumulation in green macroalgae from polar to temperate regions: Interactive effects of light versus salinity and light versus temperature. Polar Biol 12: 603–607.
15. Karsten U, Kuck K, Vogt C, Kirst GO (1996) Dimethylsulfoniopropionate production in phototrophic organisms and its physiological function as a cryoprotectant. In: Kiene, R.P., Visscher, P.T., Keller, M.D. et Kirst, G.O. (Eds.), Biological and environmental chemistry of DMSP and related sulfonium compounds. Plenum Press, New York, pp. 143–153.
16. Kirst GO (1996) Osmotic adjustment in phytoplankton and macroalgae. The use of dimethylsulfoniopropionate (DMSP). In: Kiene, R.P., Visscher, P.T., Keller, M.D. et Kirst, G.O. (Eds.), Biological and environmental chemistry of DMSP and related sulfonium compounds. Plenum Press, New York, pp. 121–129.
17. Spielmeyer A, Pohnert G. (2012) Daytime, growth phase and nitrate availability dependent variations of dimethylsulfoniopropionate in batch cultures of the diatom Skeletonema marinoi. J Exp Mar Biol Ecol 413: 121–130.
18. Sunda W, Kieber DJ, Kiene RP, Huntsman S (2002) An antioxidant function for DMSP and DMS in marine algae. Nature 418: 317–320.
19. Harada H, Vila-Costa M, Cebrian J, Kiene RP (2009) Effects of UV radiation and nitrate limitation on the production of biogenic sulfur compounds by marine phytoplankton. Aquat Bot 90:37–42.
20. Archer SD, Ragni M, Webster R, Airs RL, Geider RJ (2010) Dimethyl sulfoniopropionate and dimethyl sulfide production in response to photoinhibition in Emiliania huxleyi. Limnol Oceanogr 55: 1579–1589.
21. Dacey JWH, Wakeham SG (1986) Oceanic dimethyl sulfide: production during zooplankton grazing on phytoplankton. Science 233: 1314–1316.
22. Wolfe GV, Steinke M (1996) Grazing-activated production of dimethyl sulfide (DMS) by two clones of Emiliania huxleyi. Limnol Oceanogr 41:1151–1160.
23. Fredrickson KA, Strom SL (2009) The algal osmolyte DMSP as a microzooplankton grazing deterrent in laboratory and field studies. J Plankton Res 31 (2): 135–152.
24. Evans C, Malin G, Wilson WH, Liss PS (2006) Infectious titres of Emiliania huxleyi virus EhV-86 are reduced by exposure to millimolar dimethyl sulphide and acrylic acid. Limnol. Oceanogr. 51:2468–2471.
25. Stefels J, Dijkhuizen L (1996) Characteristics of DMSP-lyase in Phaeocystis sp. (Haptophyceae). Mar Ecol Prog Ser 131: 307–313.
26. Nguyen BC, Belviso S, Mihalopoulos N, Gostan J, Nival P (1988) Dimethyl Sulfide Production During Natural Phytoplanktonic Blooms. Mar Chem 24:133–141.
27. Leck C, Larsson U, Bagander LE, Johansson S, Hajdu S (1990) Dimethylsulfide in the Baltic Sea: annual variability in relation to biological activity. J Geophys Res 95:3353–3364.
28. Belviso S, Kim S-K, Rassoulzadegan F, Krajka B, Nguyen BC, et al. (1990) Production of dimethylsulfonium propionate (DMSP) and dimethylsulfide (DMS) by a microbial food web. Limnol Oceanogr 35: 1810–1821.
29. Malin G, Wilson WH, Bratbak G, Liss PS, Mann NH (1998) Elevated production of dimethylsulfide resulting from viral infection of cultures of Phaeocystis pouchetii. Limnol Oceanogr 43: 1389–1393.
30. Todd JD, Rogers R, Li YG, Wexler M, Bond PL, Sun L. et al. (2007) Structural and regulatory genes required to make the gas dimethyl sulfide in bacteria. Science 315: 666–669.
31. Todd JD, Curson ARJ, Dupont CL, Nicholson P, Johnston AWB (2009) The dddP gene, encoding a novel enzyme that converts dimethylsulfoniopropionate into dimethyl sulfide, is widespread in ocean metagenomes and marine bacteria and also occurs in some Ascomycete fungi. Environ Microbiol 11:1376–1385.
32. Curson ARJ, Rogers R, Todd JD, Brearley CA, Johnston AWB (2008) Molecular genetic analysis of a dimethylsulfoniopropionate lyase that liberates the climate-changing gas dimethylsulfide in several marine alpha-proteobacteria and Rhodobacter sphaeroides. Environ Microbio 10: 757–767.
33. Stefels J, Dijkhuizen L, Gieskes WWC (1995) DMSP-lyase activity in a spring phytoplankton bloom off the Dutch coast, related to Phaeocystis sp. abundance. Mar Ecol Prog Ser 123:235–243.
34. Niki T, Kunugi M, Otsuki A (2000) DMSP-lyase activity in five marine phytoplankton species: its potential importance in DMS production. Marine Biol 136:759–764.

35. Kiene RP, Linn LJ, Bruton JA (2000) New and important roles for DMSP in marine microbial communities. J Sea Res 43:209–224.
36. Vila-Costa M, Del Valle D, González JM, Slezak D, Kiene R, et al. (2006) Phylogenetic identification and metabolism of DMS-consuming bacteria in seawater. Environ Microbiol 8: 2189–2200.
37. Brimblecombe P, Shooter D (1986) Photo-oxidation of dimethylsulfide in aqueous solution. Mar Chem 19:343–353.
38. Kieber DJ, Jiao J, Kiene RP, Bates TS (1996) Impact of dimethylsulfide photochemistry on methyl sulfur cycling in the equatorial Pacific Ocean. J Geophys Res 101: 3715–3722.
39. Kettle A, Andreae M, Amouroux D, Andreae T, Bates T, et al. (1999) A global database of sea surface dimethylsulfide (DMS) measurements and a procedure to predict sea surface DMS as a function of latitude, longitude, and month, Global Biogeochem Cy 13: 399–444.
40. Lana A, Bell TG, Simó R, Vallina SM, Ballabrera-Poy J, et al. (2011) An updated climatology of surface dimethlysulfide concentrations and emission fluxes in the global ocean. Global Biogeochem Cy 25(1). Art no GB1004. doi:10.1029/2010gb003850.
41. Kiene RP, Bates TS (1990) Biological removal of dimethyl sulfide from seawater. Nature 345:702–705.
42. Simó R, Pedrós-Alió C (1999) Short-term variability in the open ocean cycle of dimethylsulfide. Glob. Biogeochem. Cycles 13: 1173–1181.
43. Le Clainche Y, Vezina A, Levasseur M, Cropp RA, Gunson JR, et al. (2010) A first appraisal of prognostic ocean DMS models and prospects for their use in climate models. Global Biogeochem Cy 24, GB3021, doi:10.1029/2009GB003721.
44. Gabric A, Murray N, Stone L, Kohl M (1993) Modeling the production of dimethylsulfide during a phytoplankton bloom. J Geophys Res Oceans 98:22805–22816.
45. Gabric A, Gregg W, Najjar R, Erickson D, Matrai P (2001) Modeling the biogeochemical cycle of dimethylsulfide in the upper ocean: a review, Chemosphere - Global Change Science 3: 377–392.
46. van den Berg AJ, Turner SM, van Duyl FC, Ruardij P (1996) Model structure and analysis of dimethylsulphide (DMS) production in the southern North Sea, considering phytoplankton dimethylsulphoniopropionate- (DMSP) lyase and eutrophication effects. Mar Ecol Prog Ser 145:233–244.
47. Laroche D, Vezina AF, Levasseur M, Gosselin M, Stefels J, et al. (1999) DMSP synthesis and exudation in phytoplankton: a modeling approach. Mar Ecol Prog Ser 180: 37–49.
48. Jodwalis CM, Benner RL, Eslinger DL (2000) Modeling of dimethyl sulfide oceanmixing, biological production and sea-to-air flux for high latitudes. J Geophys Res, 105,D11, 14,387–14,399.
49. Archer SD, Gilbert FJ, Nightingale PD, Zubkov MV, Taylor AH, et al. (2002) Transformation of dimethylsulphoniopropionate to dimethyl sulphide during summer in the North Sea with an examination of key processes via a modelling approach. Deep-Sea Res. II, 49: 3067–3101.
50. Archer SD, Gilbert FJ, Allen JI, Blackford J, Nightingale PD (2004) Modelling of the seasonal patterns of dimethylsulphide production and fate during 1989 at a site in the North Sea. Can J Fish Aquat Sci 61:765–787.
51. Lefevre M, Vezina A, Levasseur M, Dacey JWH (2002) A model of dimethylsulfide dynamics for the subtropical North Atlantic. Deep-Sea Res Part I 49:2221–2239.
52. Le Clainche Y, Levasseur M, Vézina A, Dacey JWH, Saucier FJ (2004) Behaviour ofthe ocean DMS(P) pools in the Sargasso Sea viewed in a coupled physical-biogeochemical ocean model. Can J Fish Aquat Sci 61(5): 788–803.
53. Six KD, Maier-Reimer E (2006) What controls the oceanic dimethylsulfide (DMS) cycle? A modeling approach. Global Biogeochem Cy 20, GB4011, doi:10.1029/2005GB002674.
54. Bopp L, Aumont O, Belviso S, Blain S (2008) Modeling the effect of iron fertilization on dimethylsulfide emissions in the Southern Ocean. Deep Sea Res. Part II 55, doi:10.1016/j.dsr2.2007.12.002.
55. Steiner N, Denman K (2008) Parameter sensitivities in a 1-D model for DMS and sulphurcycling in the upper ocean, Deep Sea Res. Part I 55: 847–865, doi:10.1016/j.dsr.2008.02.010.
56. Toole DA, Siegel DA, Doney SC (2008) A light-driven, onedimensional dimethylsulfide biogeochemical cycling model for the Sargasso Sea. J. Geophys. Res 113:G02009. doi:10.1029/2007JG000426.
57. Vallina SM, Simo' R, Anderson TR, Gabric A, Cropp R, Pacheco JM (2008) A dynamic model of oceanic sulphur (DMSO) applied to the Sargasso Sea: simulating the dimethylsulfide (DMS) summer paradox. J Geophys Res 113:G01009. doi: 10.1029/2007JG000415.
58. Polimene L, Archer SD, Butenschön M, Allen JI (2012) A mechanistic explanation for the Sargasso Sea DMS "summer paradox". Biogeochemistry 110: 243–255. doi: 10.1007/s10533-011-9674-z.
59. Vézina A.F. (2004) Ecosystem modelling of the cycling of marine dimethylsulfide: a review of current approaches and of the potential for extrapolation to global scales. Can J Fish Aquat Sci 61: 845–856.
60. Lancelot C, Spitz Y, Gypens N, Ruddick K, Becquevort S, et al. (2005) Modelling diatom and Phaeocystis blooms and nutrient cycles in the Southern Bight of the North Sea: the MIRO model. Mar Ecol Prog Ser 289: 63–78.
61. Stefels J, van Boekel WHM (1993) Production of DMS from dissolved DMSP in axenic cultures of the marine phytoplankton species Phaeocystis sp. Mar Ecol Prog Ser 97:11–18.
62. Liss PS, Malin G, Turner SM, Holligan PM (1994) Dimethyl sulfide and *Phaeocystis* - A Review. J Mar Syst 5:41–53.
63. Lancelot C, Mathot S (1987) Dynamics of a Phaeocystis-dominated spring bloom in Belgian coastal waters. I. Phytoplanktonic activities and related parameters. Mar Ecol Prog Ser 37: 239–248.
64. Cadée GC, Hegeman J (2002) Phytoplankton in the Marsdiep at the end of the 20th century; 30 years monitoring biomass, primary production, and Phaeocystis blooms. J Sea Res 48: 97–110.
65. Rousseau V, Leynaert A, Daoud N, Lancelot C (2002) Diatom succession, silicification and silicic acid availability in Belgian coastal waters (Southern North Sea). Mar Ecol Prog Ser 236, 61–73.
66. Lancelot C (1995) The mucilage phenomenon in the continental coastal waters of the North Sea. Sci Total Environ 165:83–102.
67. Turner SM, Malin G, Liss PS, Harbour DS, Holligan PM (1988) The seasonal variation of dimethyl sulphide and DMSP concentrations in nearshore waters. Limnol Oceanogr 33: 364–375.
68. Kwint RLJ, Kramer KJM (1996) Annual cycle of the production and fate of DMS and DMSP in a marine coastal system. Mar Ecol Prog Ser 134: 217–224.
69. Gypens N, Lacroix G, Lancelot C (2007) Causes of variability in diatom and Phaeocystis blooms in Belgian coastal waters between 1989 and 2003: a model study. J Sea Res 57: 19–35.
70. Gasparini S, Daro MH, Antajan E, Tackx M, Rousseau V, et al. (2000) Mesozooplankton grazing during the Phaeocystis globosa bloom in the Southern Bight of the North Sea. J Sea Res 43:345–356.
71. Steinke M, Daniel C, Kirst GO (1996) DMSP lyase in marine macro- and microalgae: intraspecific differences in cleavage activity. In: Kiene RP, Visscher PT, Keller MD, Kirst GO (eds) Biological and environmental chemistry of DMSP and related sulfonium compounds. Plenum Press, New York, pp 317–324.
72. Steinke M, Wolfe GV, Kirst GO (1998) Partial characterisation of dimethylsulfoniopropionate (DMSP) lyase isozymes in 6 strains of Emiliania huxleyi. Mar Ecol Prog Ser 175:215–225.
73. Steinke M, Malin G, Archer SD, Burkill PH, Liss PS (2002) DMS production in a cocclithophorid bloom: evidence for the importance of dinoflagellate DMSP lyases. Aquat Microb Ecol 26:259–270.
74. Archer SD, Widdicombe CE, Tarran GA, Rees AP, Burkill PH (2001) Production and turnover of particulate dimethylsulphoniopropionate during a coccolithophore bloom in the northern North Sea. Aquat Microb Ecol 24: 225–241.
75. Kiene RP, Linn LJ (2000) On the fate of DMSP-sulfur in seawater: tracer studies with dissolved 35S-DMSP. Geochim Cosmochim Acta 64: 2797–2810.
76. Taylor BF, Visscher PT (1996) Metabolic pathways involved in DMSP degradation. In: Kiene, R.P., Visscher, P.T., Keller, M.D., Kirst, G.O. (Eds.). Biological and Environmental Chemistry of DMSP and Related Sulfonium Compounds, Plenum, New York, pp. 265–276.
77. Kiene RP, Linn LJ, González J, Moran MA, Bruton JA (1999) Dimethylsulfoniopropionate and methanethiol are important precursors of methionine and protein-sulfur in marine bacterioplankton. Appl Environ Microbiol 65:4549–4558.
78. Simó R (2001) Production of atmospheric sulfur by oceanic plankton: biogeochemical, ecological and evolutionary links. Trends Ecol Evol 16(6):287–294.
79. Simó R, Archer SD, Pedrós-Alió C, Gilpin L, Stelfox-Widdicombe CE (2002) Coupled dynamics of dimethylsulfoniopropionate and dimethylsulfide cycling and the microbial food web in surface waters of the North Atlantic. Limnol Oceanogr 47: 53–61.
80. Zubkov MV, Fuchs BM, Archer SD, Kiene RP, Amann R, et al. (2001) Linking the composition of bacterioplankton to rapid turnover of dissolved dimethylsulfoniopropionate in an algal bloom in the North Sea. Environ Microbiol 3:304–11.
81. Zubkov MV, Fuchs BM, Archer SD, Kiene RP, Amann R, et al. (2002) Rapid turnover of dissolved DMS and DMSP by defined bacterioplankton communities in the stratified euphotic zone of the North Sea. Deep-Sea Res Part II 49:3017–3038.
82. Vila-Costa M, Simó R, Harada H, Gasol JM, Slezak D, Kiene RP (2006) Dimethylsulfoniopropionate uptake by marine phytoplankton. Science 314: 652–654.
83. Spielmeyer A, Gebser B, Pohnert G (2011) Investigations of the uptake of dimethylsulfoniopropionate by phytoplankton. ChemBioChem 12: 2276–2279.
84. Ruiz-González C, Galí M, Sintes E, Herndl GJ, Gasol JM, et al. (2012) Sunlight effects on the osmotrophic uptake of DMSP-sulfur and Leucine by polar phytoplankton. PLoS ONE 7(9): e45545. doi:10.1371/journal.pone.0045545.
85. Kiene RP (1990) Dimethylsulfide production from dimethylsulfoniopropionate in coastal seawater samples and bacterial cultures. Appl environ Microbiol 56:3292–3297.
86. Kiene R.P. (1993) Microbial sources and sinks for methylated sulfur compounds in the marine environment. In Microbial Growth on C1 Compounds, Vol. 7. Kelly, D.P., and Murrell, J.C. (eds). London, UK: Intercept, pp. 15–33Kiene, R.P., 1996. Production of methanethiol from dimethylsulfoniopropionate in marine surface waters. Mar Chem 54: 69–83.
87. Kiene RP, Linn LJ (2000) Distribution and turnover of dissolved DMSP and its relationship with bacterial production and dimethylsulfide in the Gulf of Mexico. Limnol Oceanogr 45:848–861.

88. Wolfe GV, Levasseur M, Cantin G, Michaud S (1999) Microbial consumption and production of dimethyl sulfide (DMS) in the Labrador Sea. Aquat Microb Ecol 18:197–205.
89. Zubkov M, Linn LJ, Amann R, Kiene RP (2004) Temporal patterns of biological dimethylsulfide (DMS) consumption during laboratory-induced phytoplankton bloom cycles. Mar Ecol Prog Ser 271:77–86.
90. del Valle DA, Kieber DJ, Kiene RP (2007) Depth dependent fate of biologically-consumed dimethylsulfide in the Sargasso Sea. Mar Chem 103: 197–208.
91. Brugger A, Slezak D, Obermosterer I., Herndl GJ. (1998) Photolysis of DMS in the northern Adriatic Sea dependence on substrate concentration, irradiance and DOC concentration. Mar Chem 59: 321–331.
92. Saltzman ES, King DB, Holmen K, Leck C (1993) Experimental determination of the diffusion coefficient of dimethylsulfide in water. J Geophys Res 98: 16481–16486.
93. Yang M, Blomquist BW, Fairall CW, Archer SD, Huebert BJ (2011) Air-sea exchange of dimethylsulfide in the Southern Ocean: Measurements from SO GasEx compared to temperate and tropical regions, J Geophys Res 116, C00F05, doi:10.1029/2010JC006526.
94. Gypens N, Borges AV, Lancelot C (2009) Effect of eutrophication on air–sea CO2 fluxes in the coastal Southern North Sea: A model study of the past 50 years. Global Change Biol. 15: 1040–1056.
95. Turner SM, Malin G, Nightingale PD, Liss PS (1996) Seasonal variation of dimethyl sulphide in the North Sea and an assessment of fluxes to the atmosphere. Mar Chem 54:245–262.
96. van Duyl FC, Gieskes WWC, Kop AJ, Lewis WE (1998) Biological control of short-term variations in the concentration of DMSP and DMS during a Phaeocystis spring bloom. J Sea Res 40:221–231.
97. Kiene RP, Slezak D (2006) Low dissolved DMSP concentrations in seawater revealed by small volume gravity filtration and dialysis sampling. Limnol. Oceanogr. Methods 4: 80–95.
98. Howard EC, Henriksen JR, Buchan A, Reisch CR, Bürgmann H, et al. (2006) Bacterial taxa that limit sulfur flux from the ocean. Science 314, 649–652.
99. Yoch DC (2002) Dimethylsulfoniopropionate: Its sources, role in the marine food web, and biological degradation to dimethylsulfide. Appl Environ Microbiol 68:5804–5815.
100. Slezak D, Kiene RP, Toole DA, Simó R, Kieber DJ (2007) Effects of solar radiation on the fate of dissolved DMSP and conversion to DMS in seawater. Aquat Sci 69: 377–393.
101. Vila-Costa M, Kiene RP, Simó R (2008) Seasonal variability of the dynamics of dimethylated sulfur compounds in a coastal northwest Mediterranean site. Limnol Oceanogr 53:198–211.
102. Hatton AD, Shenoy DM, Hart MC, Mogg A, Green DH (2012). Metabolism of DMSP, DMS and DMSO by the cultivable bacterial community associated with the DMSP producing dinoagellate Scrippsiella trochoidea. Biogeochemistry 110(1–3):131–146.
103. Fagerbakke KM, Heldal M, Norland S (1996) Content of carbon, nitrogen, oxygen, sulfur and phosphorus in native aquatic and cultured bacteria. Aquat Microb Ecol 10: 15–27.
104. González JM, Kiene RP, Moran MA (1999) Transformation of sulfur compounds by an abundant lineage of marine bacteria in the alpha-subclass of the class Proteobacteria. Appl Environ Microbiol 65: 3810–3819.
105. Howard EC, Sun SL, Biers EJ, Moran MA (2008) Abundant and diverse bacteria involved in DMSP degradation in marine surface waters. Environ Microb 10: 2397–2410.
106. Offre P, Spang A, Schleper C (2013) Archaea in Biogeochemical Cycles. Annu. Rev. Microbiol. 67:437–57.
107. Nightingale PD, Malin G, Law CS, Watson AJ, Liss PS, et al. (2000) In situ evaluation of air-sea gas exchange parameterizationsusing novel conservative and volatile tracers. Global Biogeochem Cy 14(1): 373–387.
108. Ho DT, Law CS, Smith MJ, Schlosser P, Harvey M, et al. (2006) Measurements of airsea gas exchange at high wind speeds in the Southern Ocean: Implications for global parameterizations. Geophys. Res. Lett., 33, L16611, doi:10.1029/2006GL026817.
109. Anderson TR, Spall SA, Yool A, Cipollini P, Challenor PG, et al. (2001) Global fields of sea surface dimethylsulphide predicted from chlorophyll, nutrients and light. J Mar Syst, 30: 1–20.
110. Aumont O, Belviso S, Monfray P (2002) Dimethylsulfoniopropionate (DMSP) and dimethylsulfide (DMS) sea surface distributions simulated from a global three dimensional ocean carbon cycle model. J Geophys Res Oceans 107(C4):3029. doi:10.1029/1999JC000111.
111. Simó R, Dachs J (2002) Global ocean emission of dimethylsulfide predicted from biogeophysical data. Global Biogeochem Cy 16: 1078.
112. Belviso S, Bopp L, Moulin C, Orr JC, Anderson TR, et al. (2004), Comparison of global climatological maps of sea surface dimethyl sulfide, Global Biogeochem Cy 18, GB3013, doi:10.1029/2003GB002193.
113. Vallina S, Simó R (2007) Strong relationship between DMS and the solar radiation dose over the global surface ocean, Science, 315, 506–508, doi:10.1126/science.1133680.
114. Lana A, Simó R, Vallina SM, Dachs J (2012) Re-examination of global emerging patterns of ocean DMS concentration. Biogeochemistry 110:173–182. DOI 10.1007/s10533-011-9677-9
115. Miles CJ, Bell TG, Suntharalingam P (2012) Investigating the inter-relationships between water attenuated irradiance, primary production and DMS(P). Biogeochemistry 110:201–213. DOI 10.1007/s10533-011-9697-5
116. Watanabe YW, Yoshinari H, Sakamoto A, Nakano Y, Kasamatsu N, et al. (2007) Reconstruction of sea surface dimethylsulfide in the North Pacific during 1970s to 2000s. Mar Chem 103: 347–358.
117. Liss PS, Watson AJ, Liddicoat MI, Malin G, Nightingale PD, et al. (1993) Trace gases and air-sea exchange. Philos Trans R Soc London A 343: 531–541.